High-efficiency Si Tandem Solar Cells and Modules for Vehicle Integrated Photovoltaics

Masafumi Yamaguchi

Toyota Tech. Inst., Nagoya, Japan

Acknowledgments: NEDO, Prof. Y. Ohshita, Prof. N. Kojima, Dr. K. Araki, Dr. K-H. Lee, Dr. D. Sato, Dr. K. Nakamura and R. Ozaki, Toyota Tech. Inst., Dr. T. Takamoto, Sharp, Dr. T. Masuda, K. Okumura, A. Satou, T. Nakado and K. Yamada, Toyota Motor, Dr. Y. Zushi and T. Tanimoto, Nissan Motor, Dr. Y. Ota and Prof. K. Nishioka, Univ. Miyazaki, M. Yamazaki and K. Kiryu, and members of the NEDO's PV-Powered Vehicle Strategy Committee.

豊田工業大学
TOYOTA TECHNOLOGICAL INSTITUTE

Outline

1. Introduction
2. Impact of High-efficiency Solar Modules on Reduction in CO_2 Emission, Charging Cost Saving and Driving Distance Increase of Electric Vehicles
3. High-efficiency and Low-cost Potential of Si Tandem Solar Cells
4. Our Recent Approaches on Si Tandem Solar Cells and Modules
5. Summary

1. Introduction

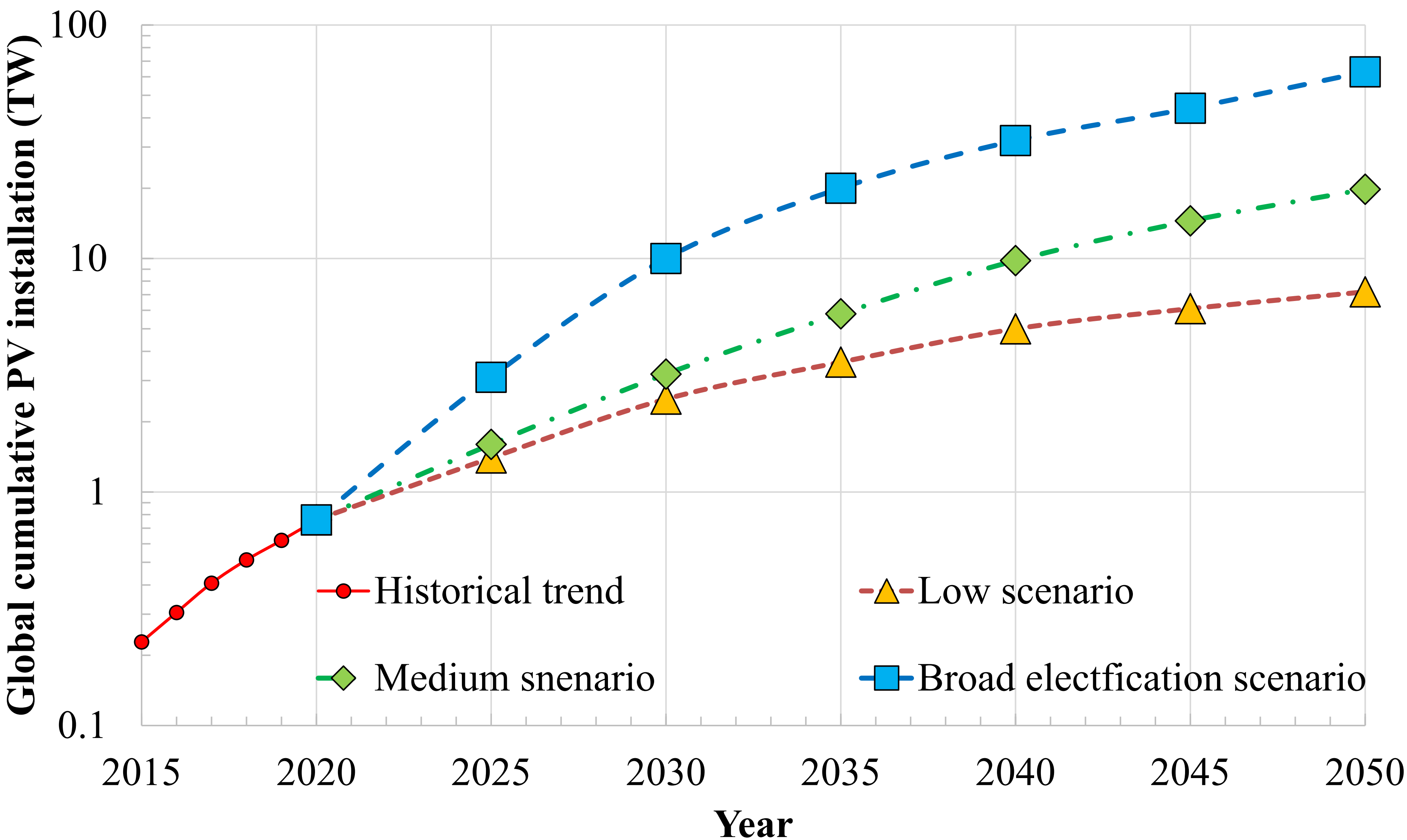

ITRPV scenario for global cumulative PV installations

(International Technology Roadmap for PV, itrpv.vdma.org)

For realizing such a vision towards creation of future clean energy infra-structures,

we need

1. to develop high performance, low cost and highly reliable PV materials, cells, modules and systems,

2. to develop smart energy management including regulations, and self-consumption in cooperation with storage battery technologies,

3. to develop new application fields such as automobile and agriculture applications towards the creation of future clean energy infrastructures.

For realizing such a vision towards creation of future clean energy infra-structures,

we need

1. to develop high performance, low cost and highly reliable PV materials, cells, modules and systems,

2. to develop smart energy management including regulations, and self-consumption in cooperation with storage battery technologies,

3. to develop new application fields such as automobile and agriculture applications towards the creation of future clean energy infrastructures.

2. Impact of High-efficiency Solar Modules on Reduction in CO_2 Emission, Charging Cost Saving and Driving Distance Increase of Electric Vehicles

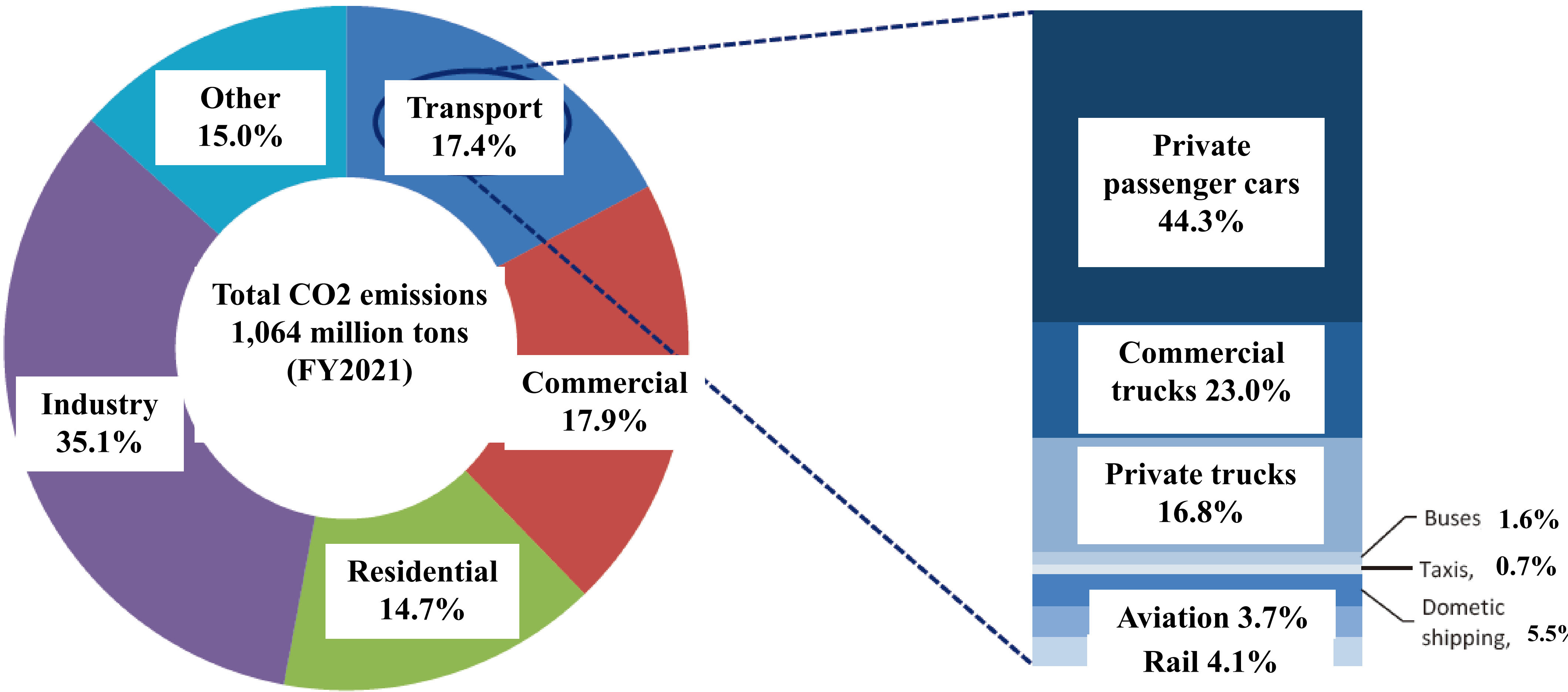

Breakdown of CO_2 emissions in transport sector in Japan

NEDO's Interim Report "PV-Powered Vehicle Strategy Committee" released on Jan. 31st 2018. Updated

CO_2 Emission in Japan

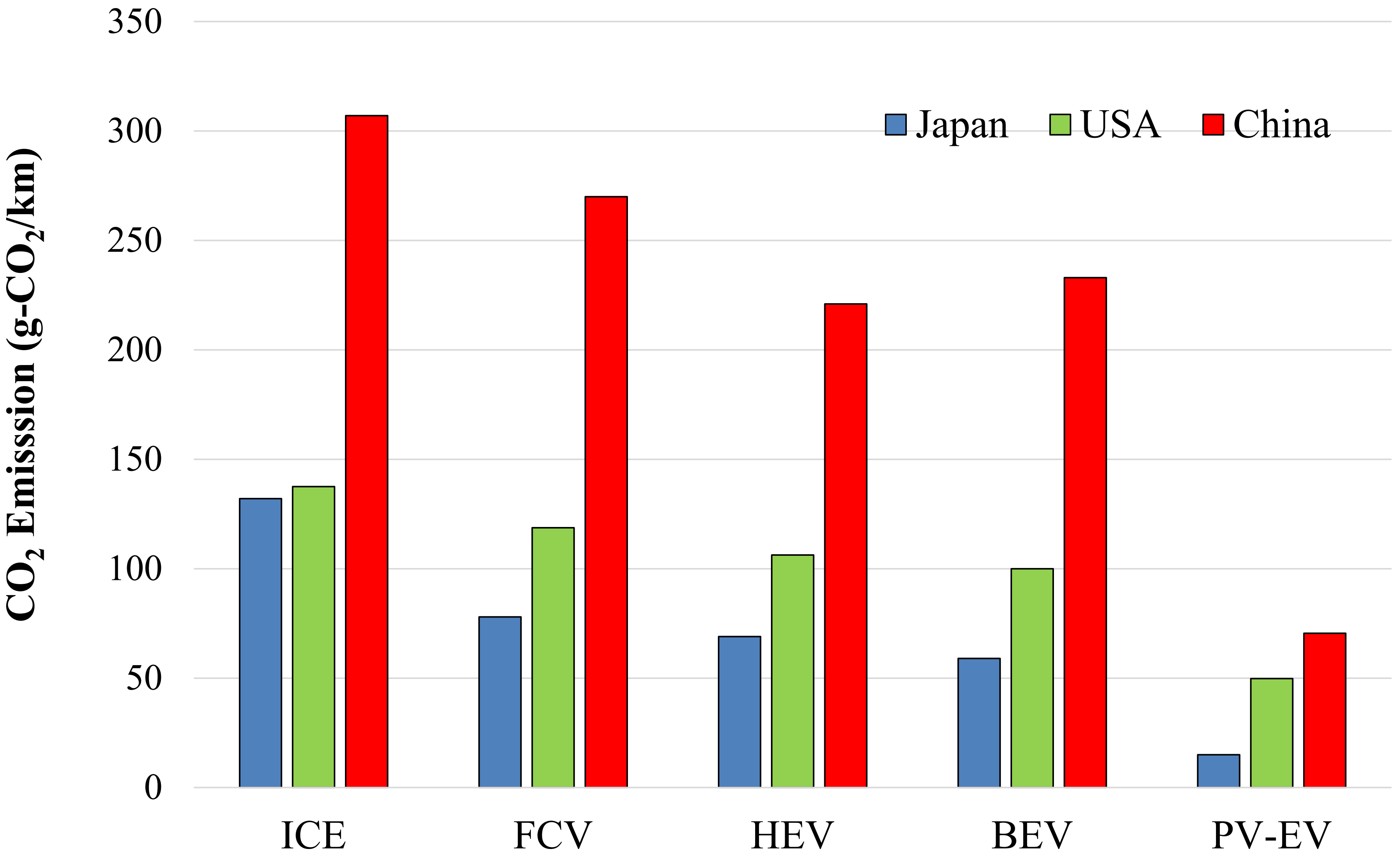

CO_2 emission per 1km driving for various vehicles in Japan, USA and China.

Renewable Energy Institute, “Trends and Prospect of EV”, 2018.6, www.renewable-ei.org.

M. Yamaguchi et al., Energy and Power Engineering **12**, 375 (2020).

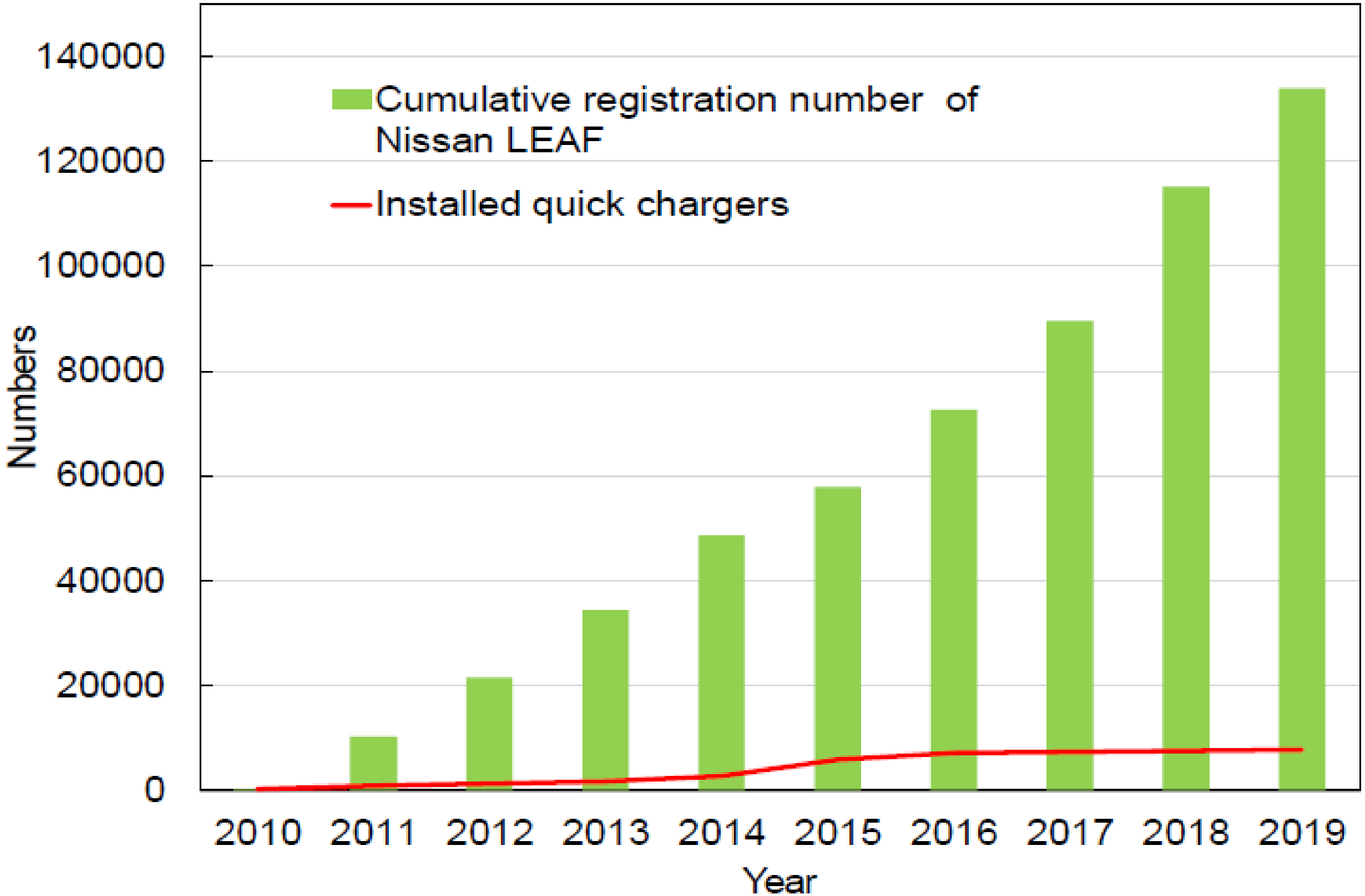

Changes in cumulative registration number of Nissan LEAF (BEV) and number of quick chargers installed.

Japan automobile dealers association, http://www.jada.or.jp/data/month/m-brand-ranking/CHAdeM Association (2016), https://www.chademo.com/wp2016/wp-content/japan-uploads/QCkasyosuii.pdf

M. Yamaguchi et al., Energy and Power Engineering **12**, 375 (2020).

Prediction of a number of PV-powered vehicles

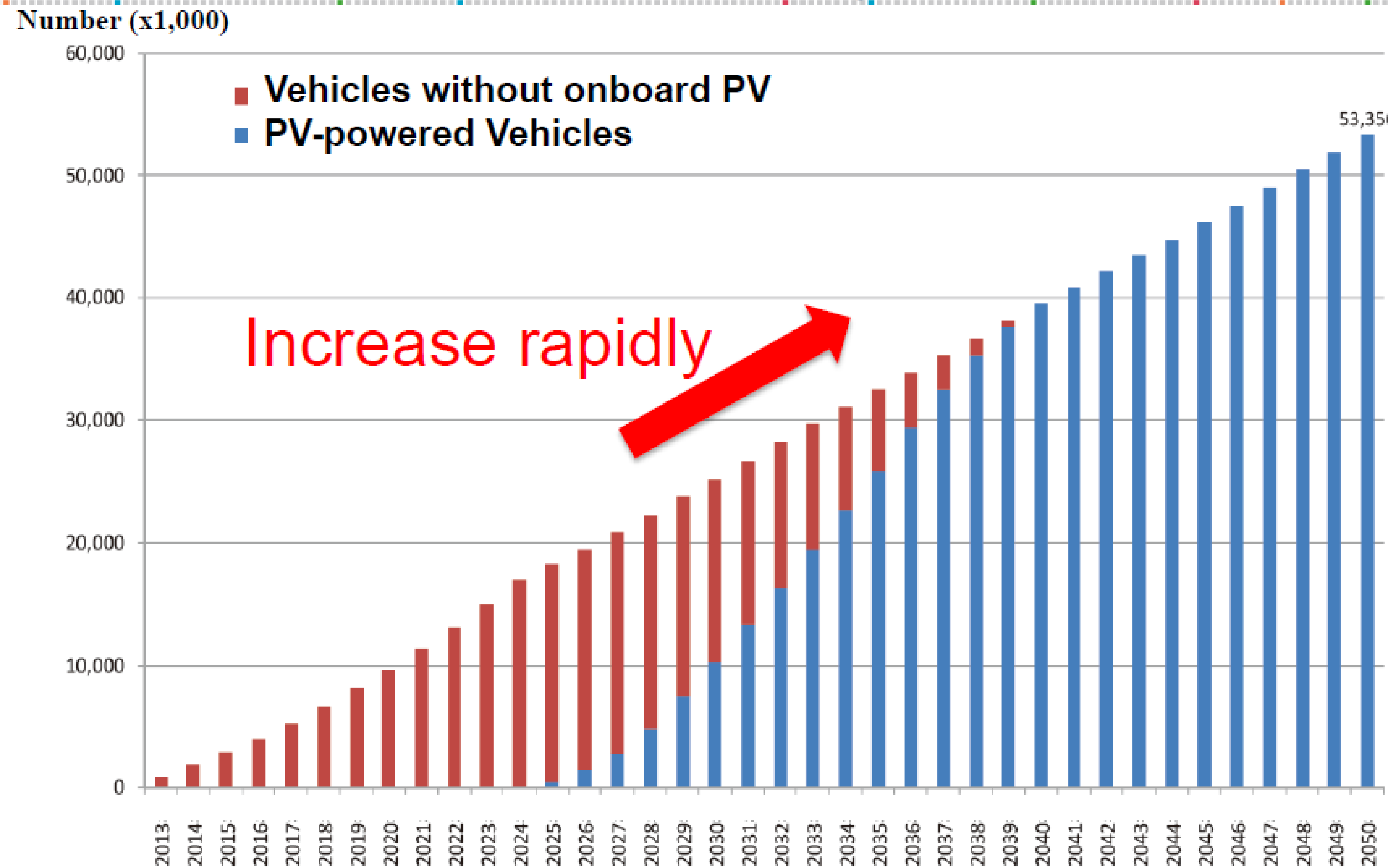

NEDO's Interim Report "PV-Powered Vehicle Strategy Committee" released on Jan. 31st 2018.

https://www.nedo.go.jp/english/news/AA5en_100358.html

Large market growth of PV and transport sector use in the USA

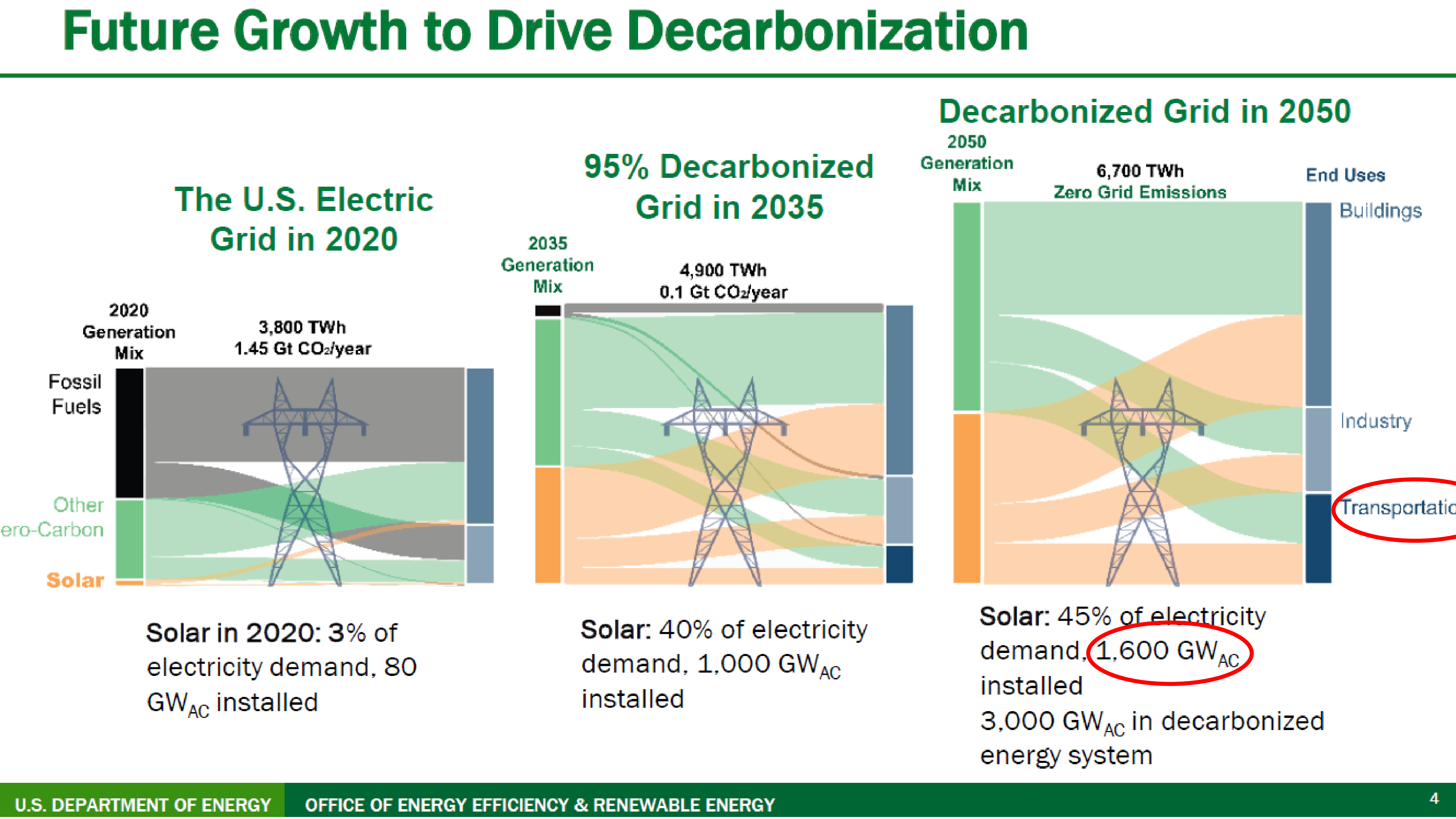

Becca Jones-Albertus, presented at the 49th IEEE PVSC, Philadelphia, June 2022

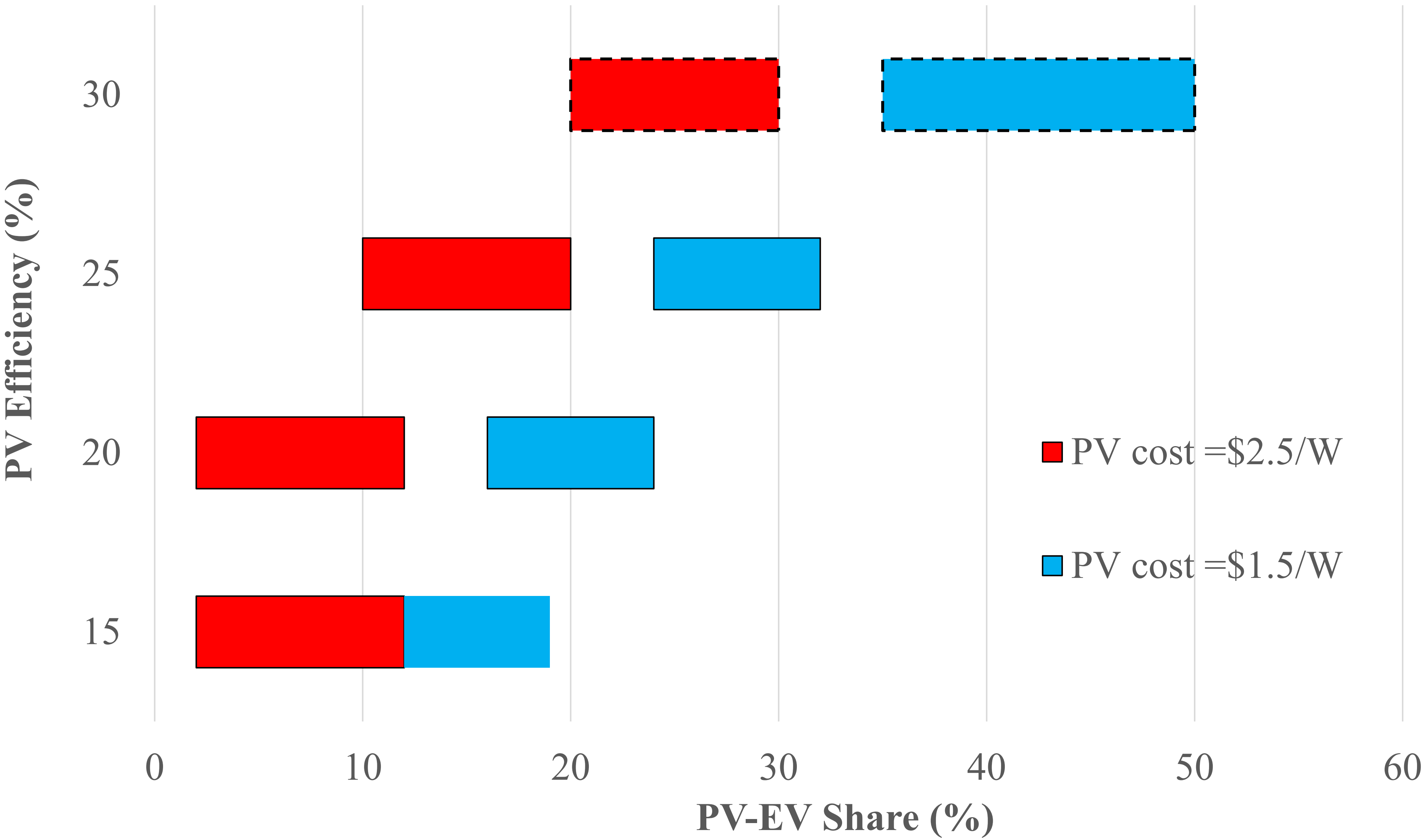

PV efficiency and cost impact on PV-EV applications estimated from the survey reports.

T. Hara et al., SAE Technical Paper 2016-01-1286, 2016, doi:10.4271/2016-01-1286.

Necessity of high-efficiency PV modules for VIPV

How to install 800 W modules?

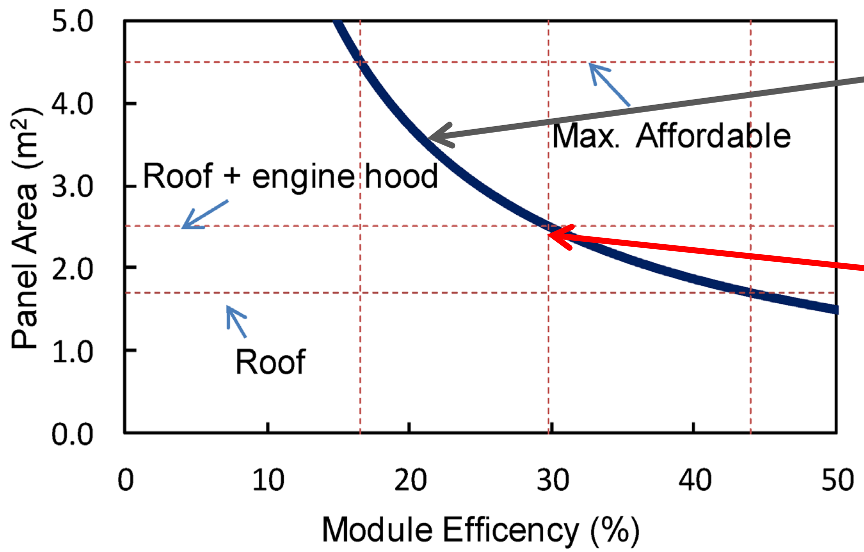

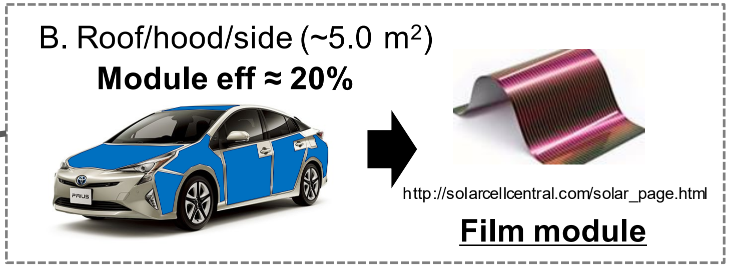

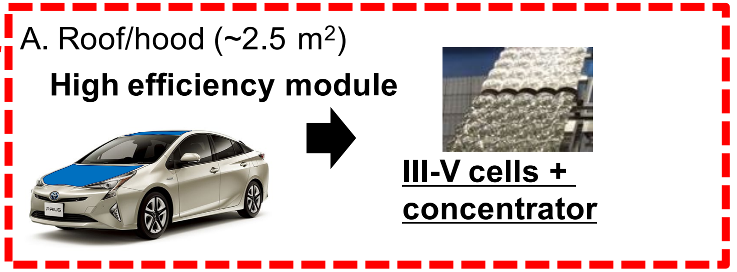

T. Masuda et al., Solar Energy **146**, 523 (2017).

Comparison of Toyota Prius and Nissan Van demonstration cars. .

Model	Toyota Prius demonstration car	Nissan Van demonstration car
Photo		
Vehicle	PHEV	BEV
Solae Cell	InGaP/GaAs/InGaAs 3-junction solar cell	InGaP/GaAs/InGaAs 3-junction solar cell
Module efficiency	More than 30%	More than 30%
Installed area	Roof, hood, back door	Roof, hood, rear gate
Output power	860 W	1150 W
Battery capacity	8.8 kWh	40 kwh
Electric mileage	~9.35 km/kWh	~6.6 km/kWh

M. Yamaguchi et al., presented at the 50th IEEE PVSC, Puerto Rico, June 11-16, 2023.

Test driving of the Toyota Prius PHV demonstration car at the Tokyo Ginza, Nov. 15, 2019.

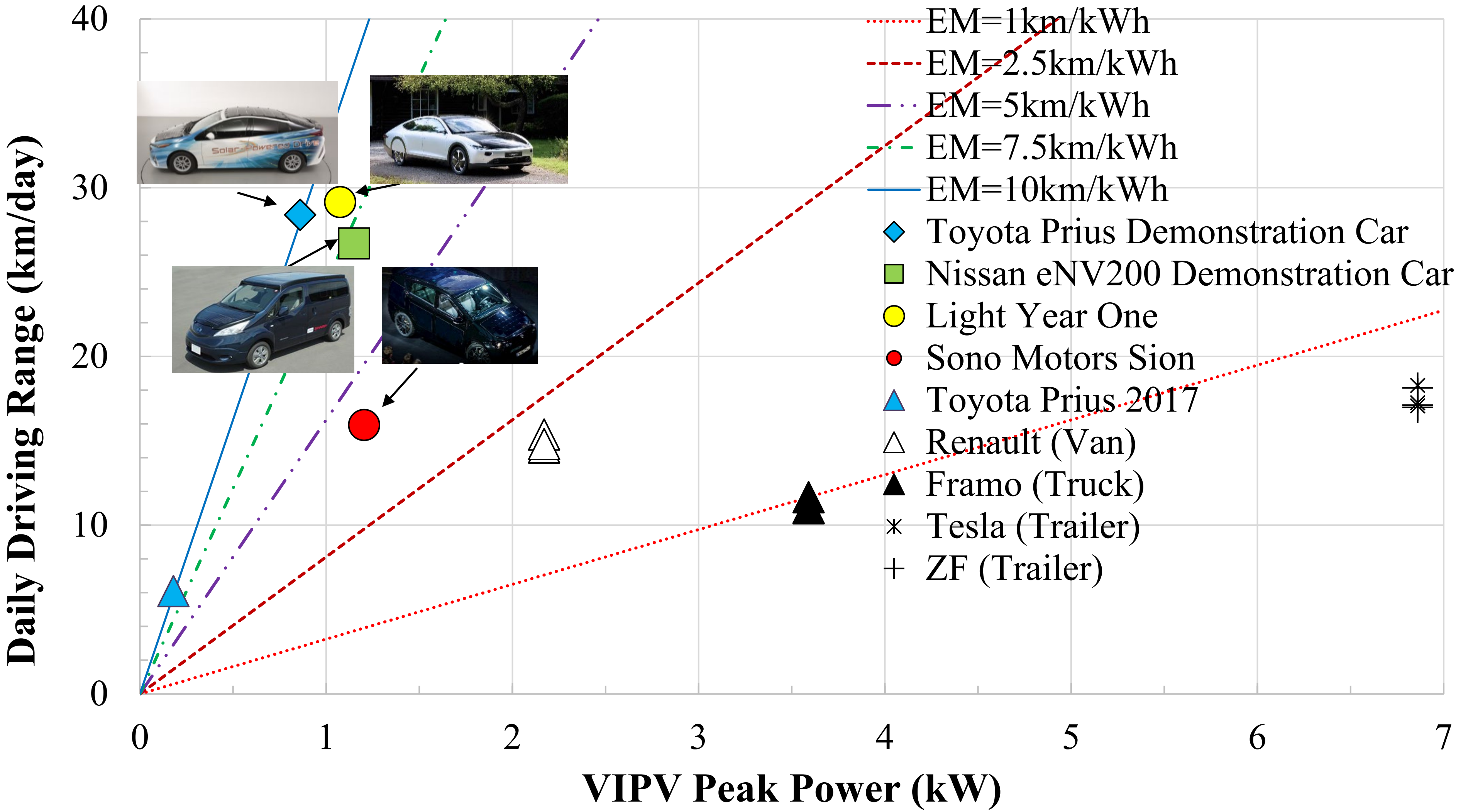

Calculated results for changes in daily driving distance of PV-powered vehicles as a function of VIPV peak power in comparison with calibrated actual data for various PV-powered vehicles.

M. Yamaguchi et al., Prog. Photovolt. **29**, 684 (2021).

T. Miyoshi, J. of Jpn. Soc. Appl. Electromagnetics, **25**, 379 (2017).

Sono Motors, https://sonomotors.com/en/sion/. Lightyear, https://lightyear.one/lightyear-one.

Y. Tomita et al., 5th International Electric Vehicle Technology Conference (EVTech 2021) .

Effects of introduction of high-efficiency solar cell modules into EVs upon reduction in CO_2 emission were analysed.

Average CO_2 emission intensity CI_{EV} for EVs reported is 462 g-CO_2 e/kWh.

EV usage CO_2 emission CE_{EV} is expressed by

CE_{EV}[g-CO_2 e/km] = CI_{EV}[g-CO_2 e/Wh]EC_{EV}[Wh/km]) = CI_{EV}[g-CO_2 e/Wh]/EM[km/Wh]), (1)

where EC_{EV} is the EV energy consumption and EM is the electric mileage.

On the other hands, CO_2 emission $CE_{PV\text{-}production}$ for PV-production is given by

$CE_{PV\text{-}production}$[g-$CO_2$ e/km] = P_{pv}[W]CI_{PV}[g-CO_2 e/W]/(DD [km/day]τ_{PV} [years]), (2)

where P_{pv} is the module output power, CI_{PV} is the carbon intensity per unit W, DD is the driving distance, and τ_{PV} is the lifetime for PV modules.

In this study, 1,008 g-CO_2 e/W was assumed as CI_{PV} according to the reference and 15 years were assumed as τ_{PV} because of PV-powered vehicle applications. The PV-EV usage CO_2 emission $CE_{PV\text{-}EV}$ is expressed by

$CE_{PV\text{-}EV}$[g-CO_2 e/km] = CE_{EV}[g-CO_2 e/km] + $CE_{PV\text{-}production}$ [g-CO_2 e/km]. (3)

M. Yamaguchi et al., Energy and Power Engineering **13**, 147 (2021).

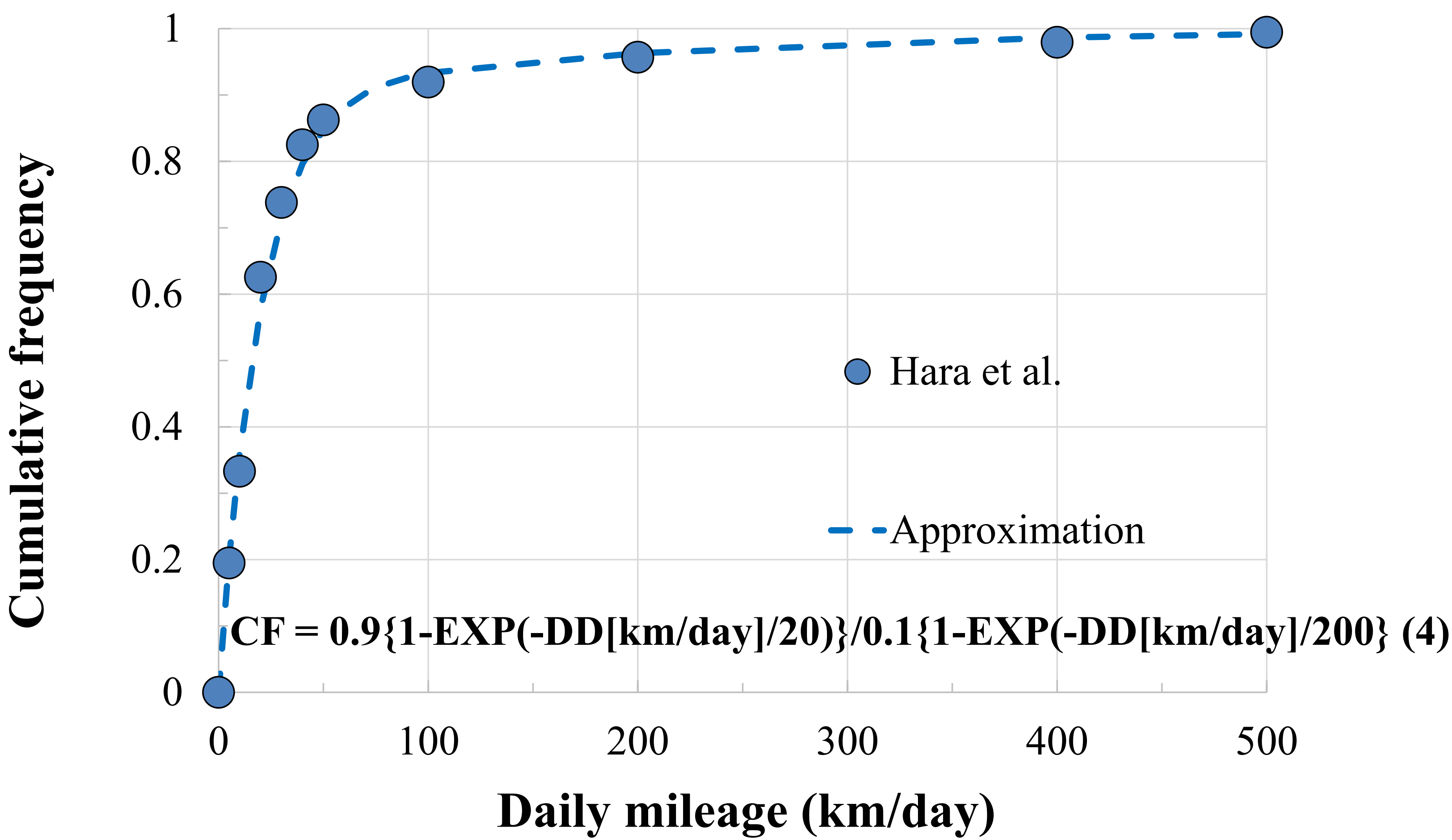

Changes in cumulative frequency of passenger cars in Japan as a function of daily mileage reported in the reference (Hara et al.) and approximation curve.

M. Yamaguchi et al., Energy and Power Engineering **13**, 147 (2021).

Driving distance DD was estimated by using the following equation:

$DD[km/day] = SI[kWh/m^2/day] PR * \eta[\%] * 0.01 A [m^2] EM[km/kWh]$, (5)

where SI is the solar irradiance, PR the performance ratio of PV system and 0.739 was used as the PR in this case, A is the area of solar cell module and 3 m^2 was used as A this time, and EM is the electric mileage.

In the calculation, sharing ration of EV mode and PV mode for PV-EV was estimated by driving distance DD and eqs. (1) – (5).

M. Yamaguchi et al., Energy and Power Engineering **13**, 147 (2021).

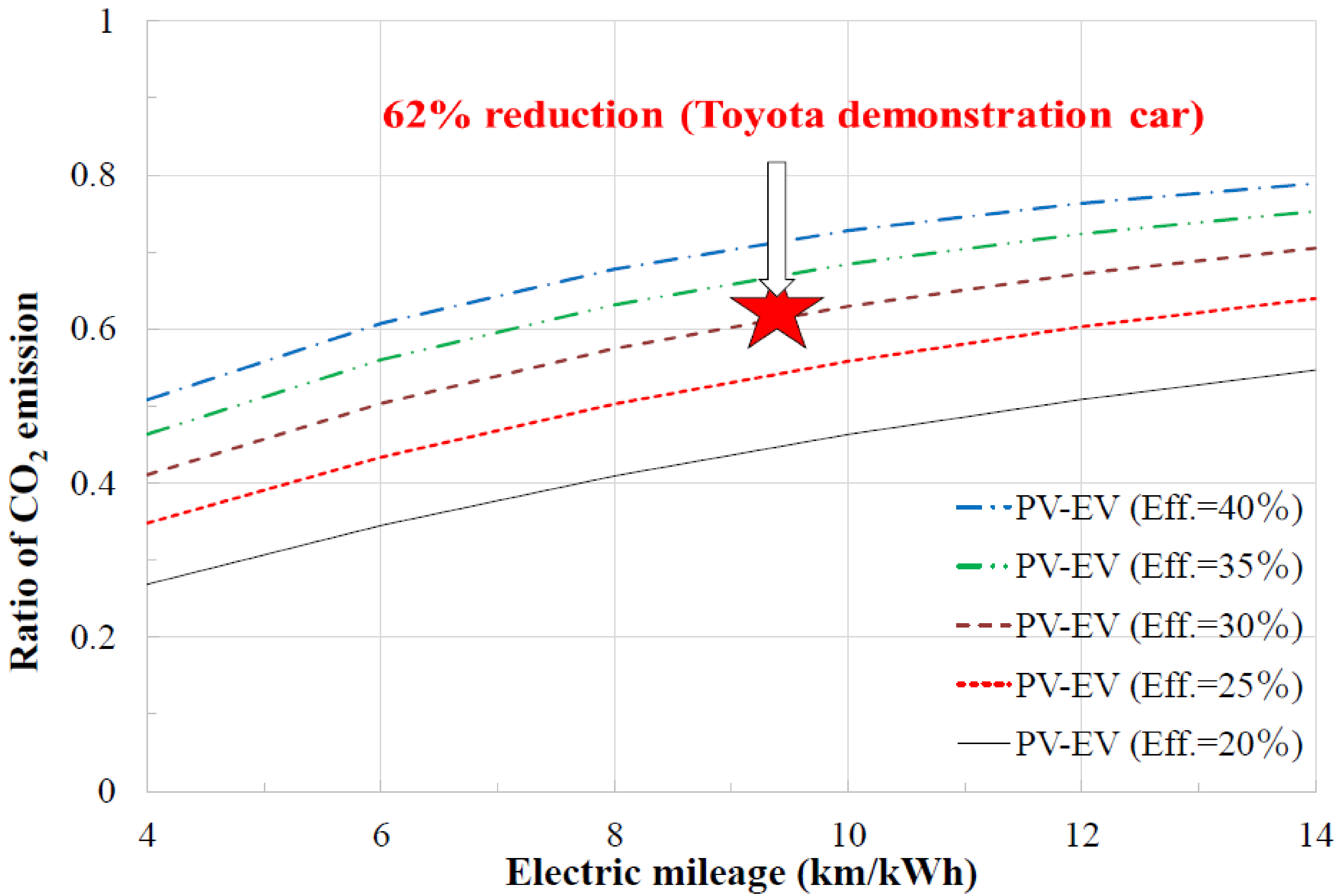

Calculated results for reduction ratio of CO_2 emission of PV-EV installed with solar cell modules with different efficiencies as a function of electric mileage EM.

M. Yamaguchi et al., IEEE J-PV **13**, 343 (2023).

Electricity cost saving for EV charging by usage of PV was analysed in this study. EV energy consumption EC is given by

EC [kWh/year] = DD [km/year]/EM [km/year]. (6)

Charging electricity cost CC of EV charging is given by

CC [$/year] = EC [kWh/year]* EP [$/kWh], (7)

where EP is the household electricity and is $0.207/kWh in Japan in 2020. PV-EV cost saving $\Delta CS_{PV\text{-}EV}$ was calculated by using the following equation

$$\Delta CS_{PV\text{-}EV}\ [\$/year] = -\Delta E_{grid}\ [kWh/year] * EP\ [\$/kWh]. \quad (8)$$

M. Yamaguchi et al., Energy and Power Engineering **13**, 147 (2021).

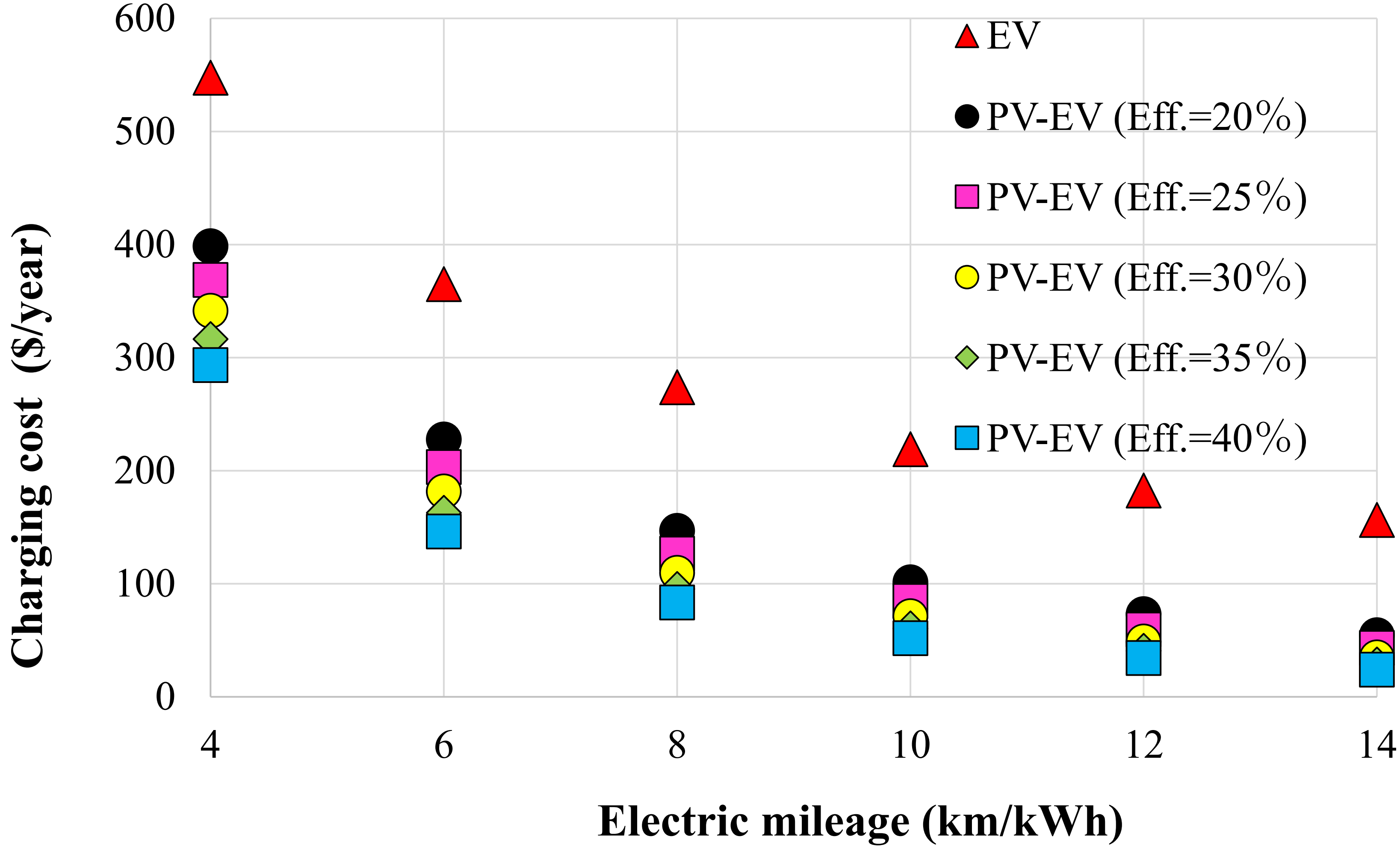

Calculated results for charging electricity cost of EV and PV-EV as a function of electric millage by assuming 30 km/day as average daily driving distance.

M. Yamaguchi et al., Energy and Power Engineering **13**, 147 (2021).

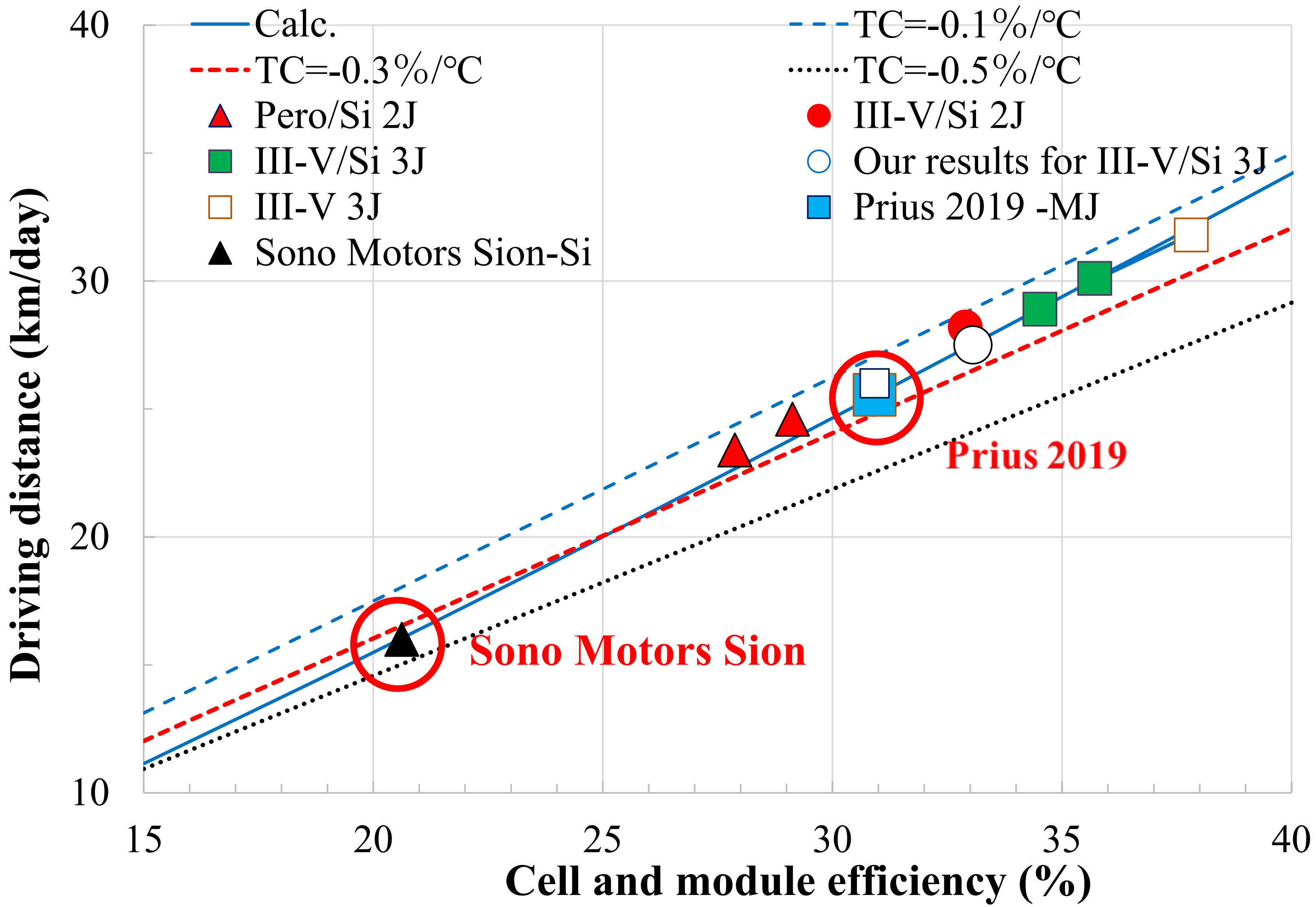

Calculated results for driving distance of vehicles powered by various Si tandem solar cells and III-V 3-junction tandem solar cells and module as a function of cell and module efficiency and temperature coefficient (TC) in comparison with estimated values of vehicles powered by various solar cells and module and actual driving distance calibrated of the Prius 2019 powered by 3-junction solar cell module and the Sono Motors Sion powered by back-contact Si solar cell module.

M. Yamaguchi et al., Solar RRL **6,** 2100429 (2022).

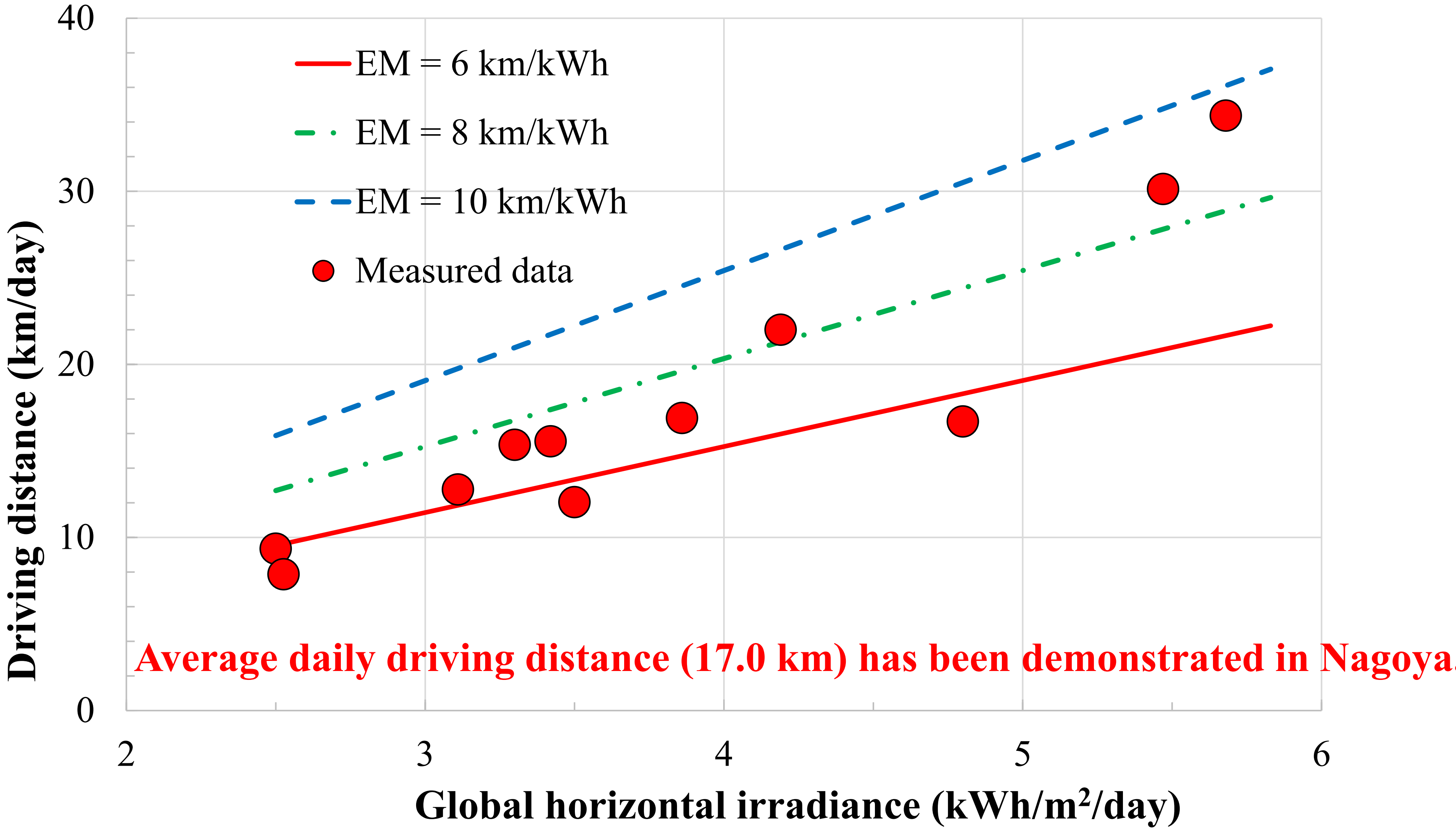

Calculated and actual driving distance for the Toyota Prius demonstration car with various EMs as a function of solar irradiance (GHI).

M. Yamaguchi et al., IEEE J. Photovolt. **13**, 343 (2023).

Kings's expression for temperature rise: $\triangle T = T_m - T_0 = SI*EXP[a + b*v]$

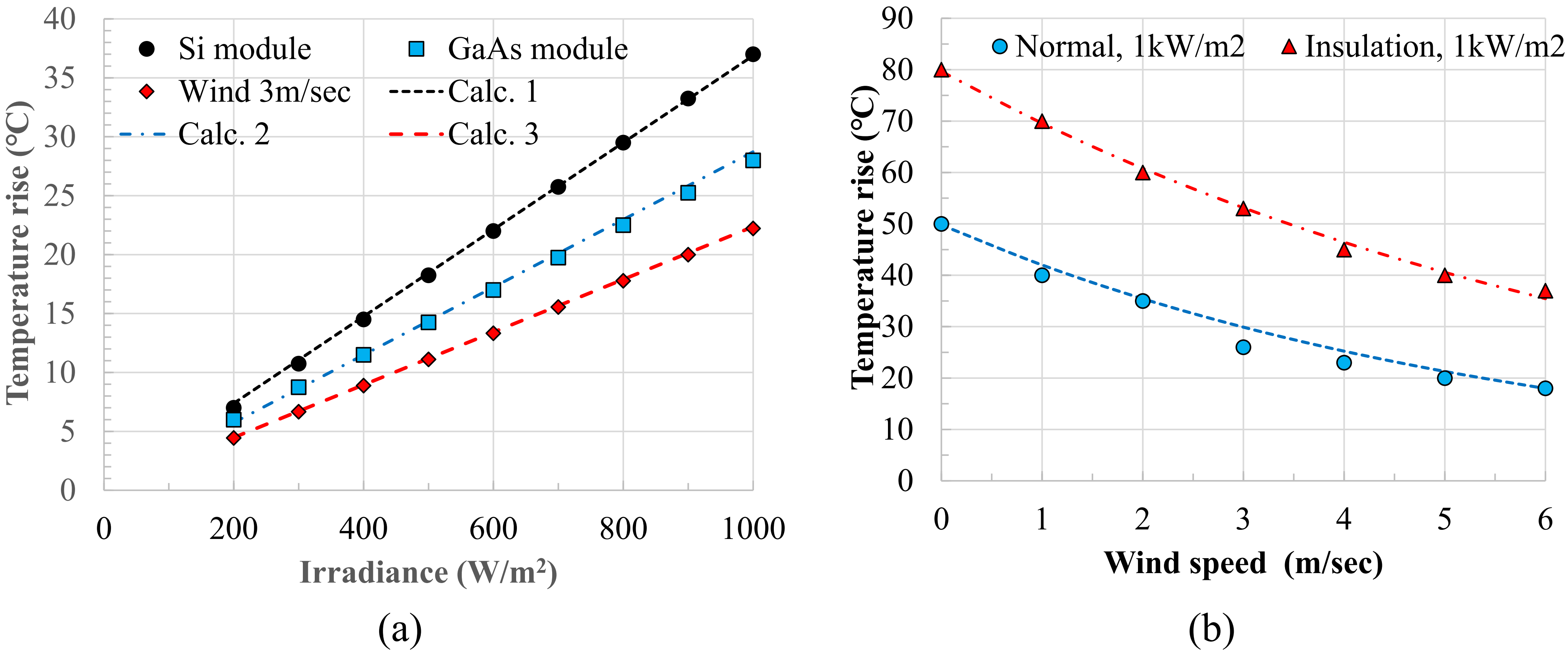

(a) Temperature rise (measured temperature above ambient temperature) of Si module and GaAs module in the case of wind speed of 0.75-1.25 m/sec and Si module in the case of 3 m/sec as a function of solar irradiation, (b) temperature rise of crystalline Si solar cell modules with and without insulation as a function of wind speed.

Data from A. Wheeler et al., Proc. 47th IEEE PVSC (IEEE, New York, 2019) p.894.

M. Yukawa et al., , Trans. IEE Japan. **116-B**, 1101 (1996) (in Japanese).

Calculations were made by King's expression (Photovoltaic array performance model, Sandia Report: SAND2004-3535, 2004).

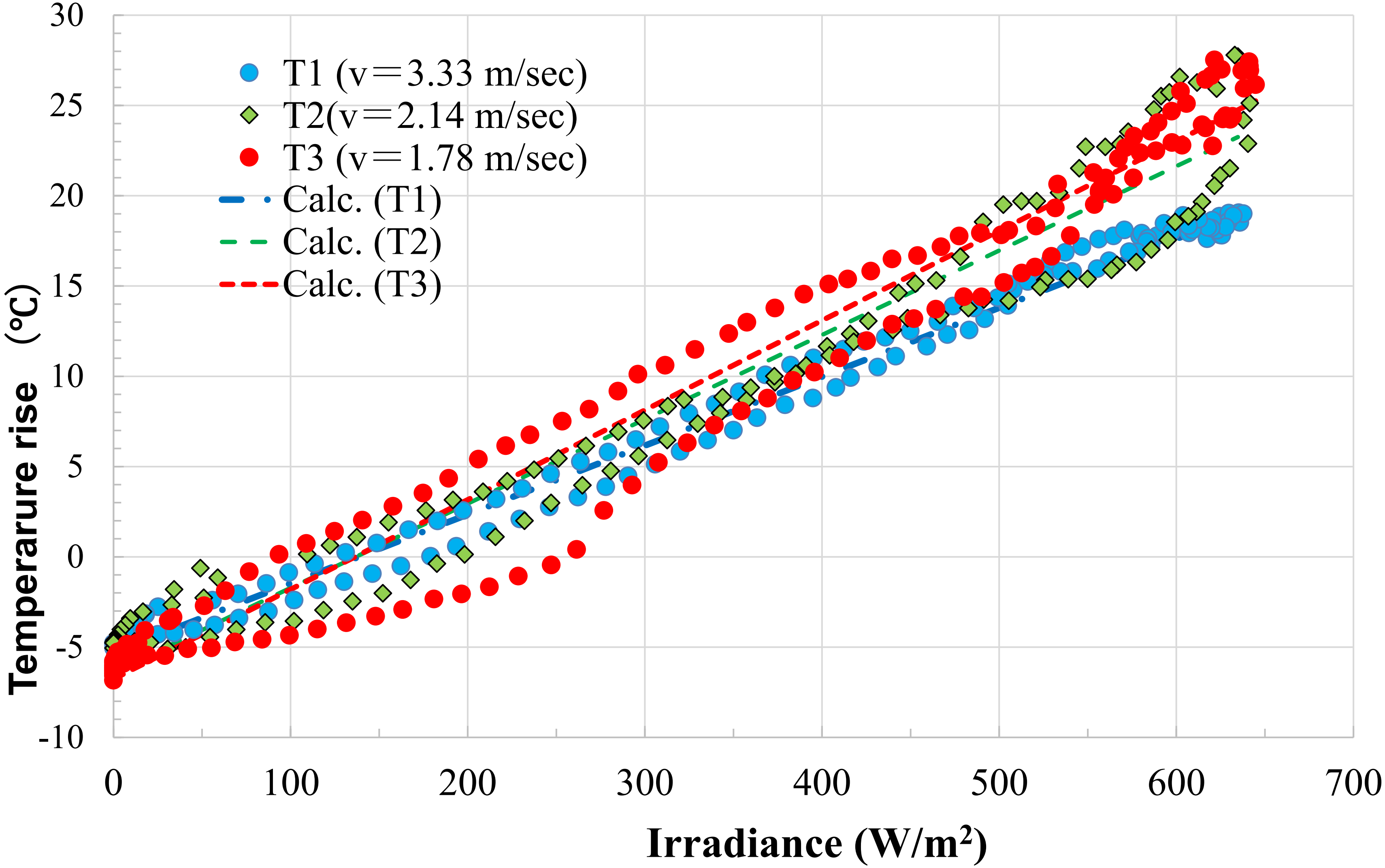

Our data for the temperature rise of solar cell modules versus solar irradiance in the 3 cases of average wind speed.

M. Yamaguchi et al., presented at the 50th IEEE PVSC Puerto Ric., June 2023.

$\triangle T_L = T_m - T_0 = c*EXP[d*v] = -9*EXP[-0.16v]$ $\triangle T/SI = EXP[a + b*v] = EXP[-2.7 - 0.17v]$

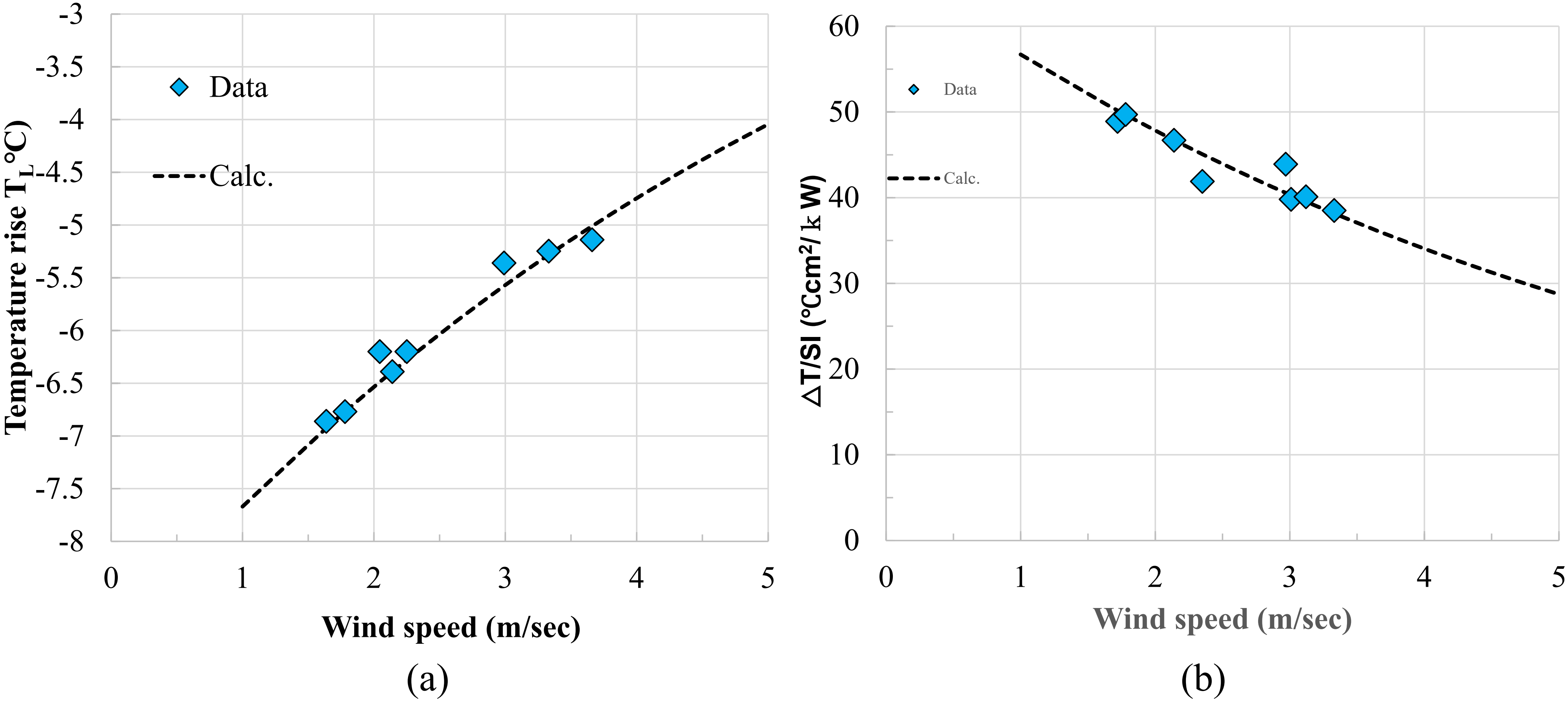

(a) temperature rise of solar cell modules under zero solar irradiance $\triangle T_L$ versus wind speed, (b) temperature rise $\triangle T$ relative to solar irradiance SI of solar cell modules under normal solar irradiation conditions versus wind speed.

M. Yamaguchi et al., presented at the 50th IEEE PVSC Puerto Ric., June 2023.

Total temperature rise ΔT_T of solar cell modules is given by

$$\Delta T_T = \Delta T_L + \Delta T = c*EXP[d*v] + SI*EXP[a + b*v], (1)$$

where T_m is the module temperature [℃], T_0 is the ambient temperature [°C], SI is the solar irradiation incident on the module surface [W/m^2], and v is the wind speed [m/sec].

a is the empirically-determined coefficient establishing the upper limit for module temperature at low wind speed and high solar irradiation,

b is the empirically-determined coefficient establishing the rate at which module temperature decreases as wind speed increases,

c is the empirically-determined coefficient establishing the upper limit for module temperature decrease at low wind speed under zero solar irradiation

d is the empirically-determined coefficient establishing the rate at which module temperature decreases as wind speed decreases.

M. Yamaguchi et al., presented at the 50^{th} IEEE PVSC Puerto Ric., June 2023.

Empirically determined coefficients were used to predict module temperature for various solar cell modules including our solar cell module.

Module type	Mount	a	b	c	d	Reference
Si module Slide 7 (a)	close mount	-3.05	-0.25	0		Wheeler et al.
GaAs module (a)	close mount	-3.05	-0.5	0		Wheeler et al.
Si module under wind speed with 3m/sec (a)	close mount	-3.05	-0.25	0		Yukawa et al.
Si module Slide 7 (b)	insulated	-2.53	-0.135	0		Yukawa et al.
Si module (b)	Standard (close mount)	-3	-0.17	0		Yukawa et al.
Our module	insulated	-2.7	-0.17	-9	-0.6	This study

Ref. : D.L. King et al., W.E. Photovoltaic array performance model, Sandia Report: SAND2004-3535. Sandia National Laboratories, 2004.

M. Yamaguchi et al., presented at the 50th IEEE PVSC Puerto Ric., June 2023.

Driving distance DD was estimated by using the following equation:

$$DD[km/day] = SI[kWh/m^2/day]*SE*\eta[\%] *(1-TC*\triangle T)*A\,[m^2]*EM[km/kWh], \quad (2)$$

where SI is the global solar irradiation, SE is the efficiency of the PV system (according to our previous study, 0.739 was used in this study), η is the efficiency of the solar cell module, TC is the temperature coefficient of solar cell module, ΔT is the temperature rise of solar cell module, A is the area of solar cell module, and EM is the electric mileage of the PV-EV.

Calculations were carried out by using eqs. (2) and (1), and parameters shown in previous table and assuming -0.3%/°C as the temperature coefficient TC of VIPV modules.

In the calculation, 1 kW was used as the output power of the VIVP module, and 10 km/kWh was assumed as EM.

M. Yamaguchi et al., presented at the 50th IEEE PVSC Puerto Ric., June 2023.

World map and the major cities analyzed in the world.

M. Yamaguchi et al., presented at the 50th IEEE PVSC Puerto Ric., June 2023.

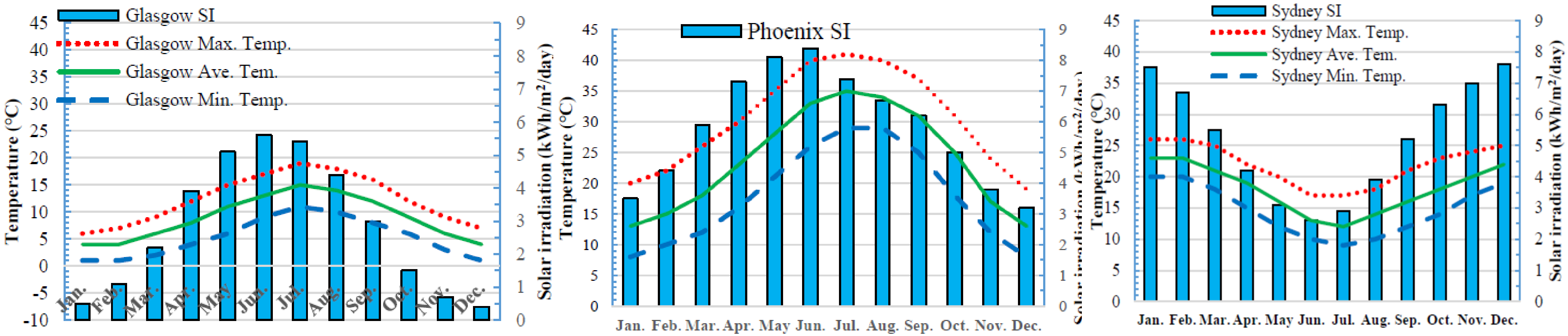

(a)

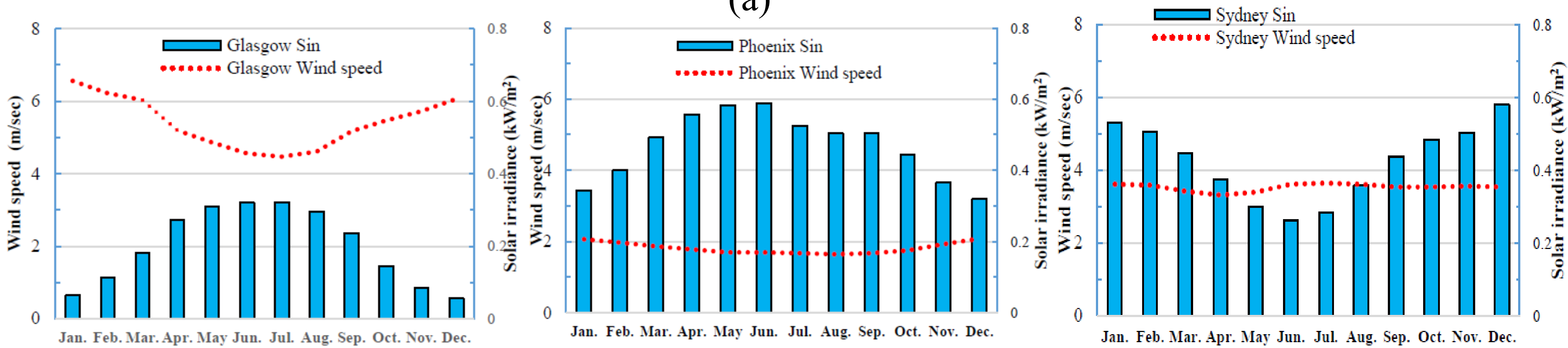

(b)

Examples for (a) daily average global solar irradiation [kWh/m²/day], monthly maximum, average, and minimum ambient temperature [°C], (b) average solar irradiance [kW/m²] and average wind speed [m/sec] in the major cities in the world. M. Yamaguchi et al., presented at the 50th IEEE PVSC Puerto Ric., June 2023.

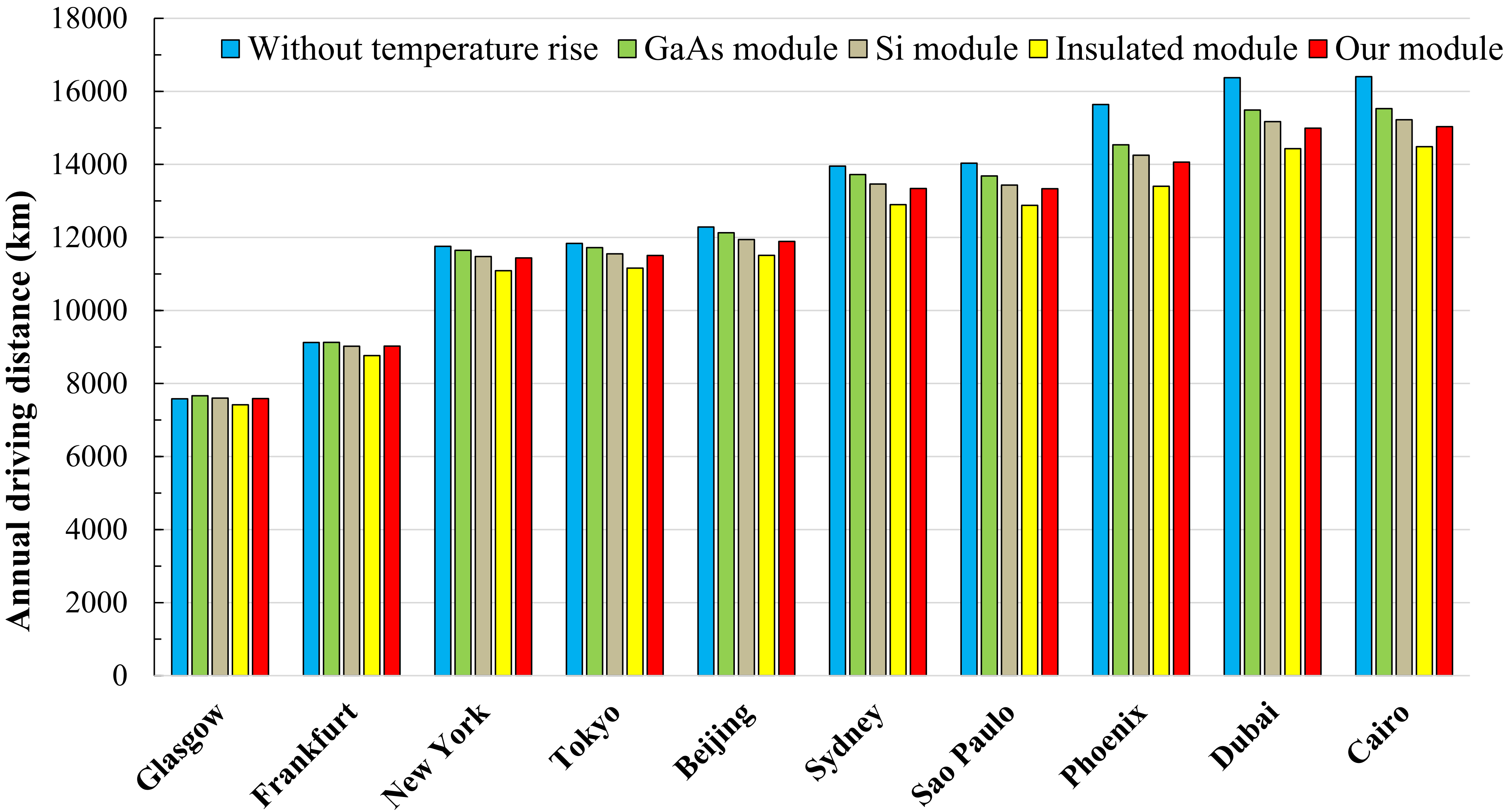

Annual driving distances calculated by considering power loss due to the temperature rise of solar cell modules and the effects of wind speed for PV-EV installed with 1 kW VIVP module and EM of 10 km/kWh under driving in major cities in the world.

M. Yamaguchi et al., presented at the 50th IEEE PVSC Puerto Ric., June 2023.

Annual driving ranges were estimated by considering the effects of temperature rise of VIPV modules for the Toyota Prius and Nissan Van demonstration cars and the actual annual driving range

Car	Location	Annual driving range (km)			Additional power loss
		Estimated range without temperature rise	Estimated range with temperature rise	Actual annual driving range	
Toyota Prius test car (VIPV power =860W, EM =9.35km/kWh)	Nagoya	9,718	9,114	6,211	31.9%
Nissan Van test car (VIPV power =1150W, EM =6.6km/kWh)	Yokohama	9,054	8,502	7,090	16.6%

M. Yamaguchi et al., presented at the 50th IEEE PVSC Puerto Ric., June 2023.

Ppower loss was calculated by using eqs. (2) (3) and maximum outside temperature T_{max}. .

$EM=EM_0(19-T_{max})x(\pm 0.4)$ [km/kWh/°C], (2)

$EM=EM_0(19-T_{max})x (\pm 0.2)$ [km/kWh/°C], (3)

where EM_0 is the original EM of PV-EV in the case of no operation of air-conditioners.

Such values are fitted with experimental values, although the reference value is about -0.25 km/kWh/°C.

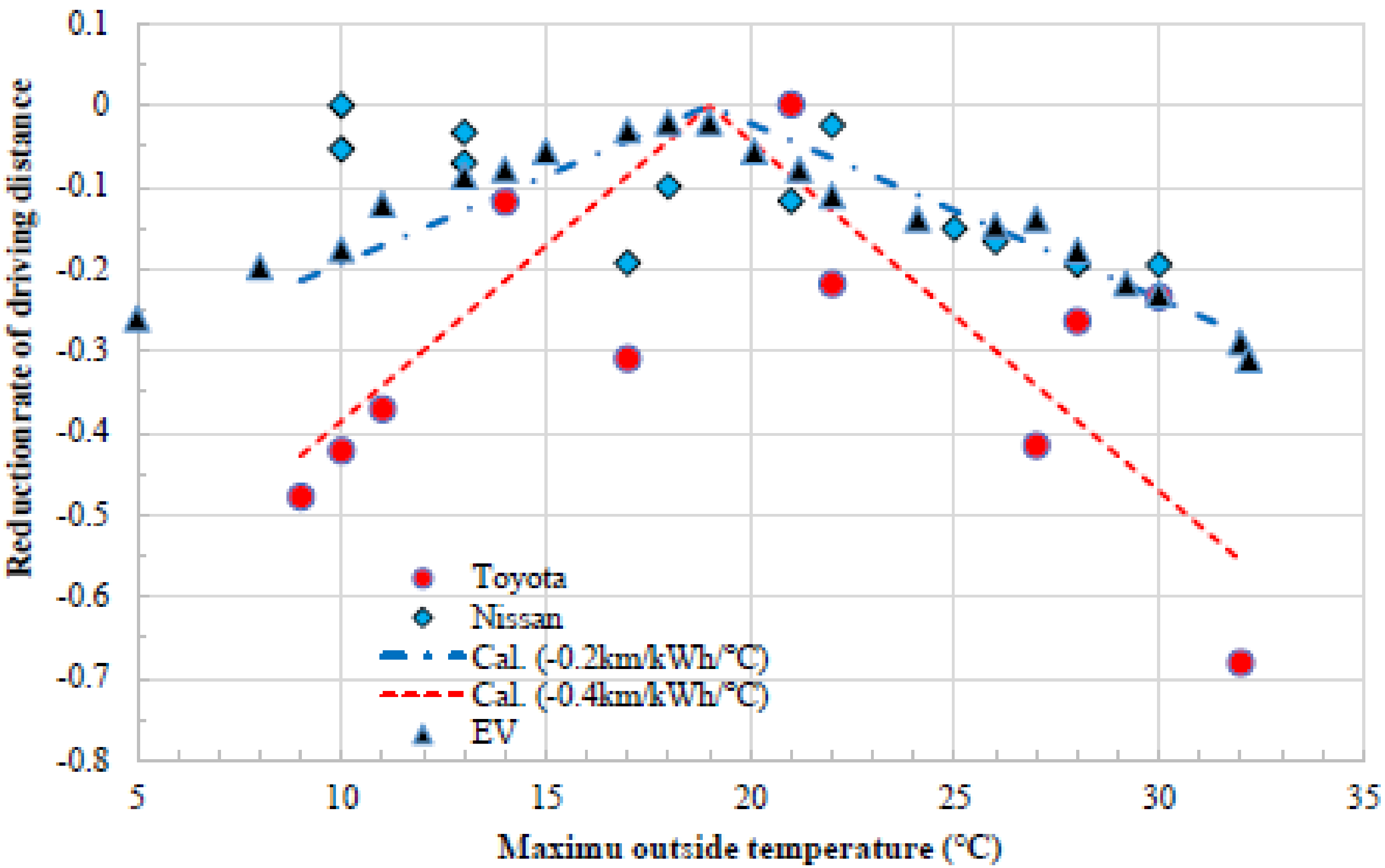

Reduction ratio of driving distance of the Toyota Prius demonstration car and the Nissan Van demonstration car during one year driving due to usage of air-conditioner versus maximum outside temperature during one month driving and calculated reduction ratio of driving distance.

M. Yamaguchi et al., presented at the 40th EU-PVSEC Lisbon, Sep. 2023.

Driving distance of PV-EV in the major cities in Japan and the world as a result of usage of air-conditioner was analyzed by using eq. (4) and (5).

$$DD[km/day]=SI[kwh/m^2/day] x SE x \eta[\%] x A[m^2] x EM_0 (19-T_{max}) x (\pm 0.2) [km/kWh/°C], \quad (4)$$

$$DD[km/day]=SI[kwh/m^2/day] x SE x \eta[\%] x A[m^2] x EM_0 (19-T_{max}) x (\pm 0.4) [km/kWh/°C], \quad (5)$$

where 1kW was used as output power of VIVP module, 0.739 was assumed as SE and 10 km/kWh was assumed as EM_0.

M. Yamaguchi et al., presented at the 40th EU-PVSEC Lisbon, Sep. 2023.

Japan map- Sapporo, Sendai, Niigata, Tokyo, Yokohama, Nagoya, Osaka, Hiroshima. Kochi, Miyazaki

M. Yamaguchi et al., presented at the 40th EU-PVSEC Lisbon, Sep. 2023.

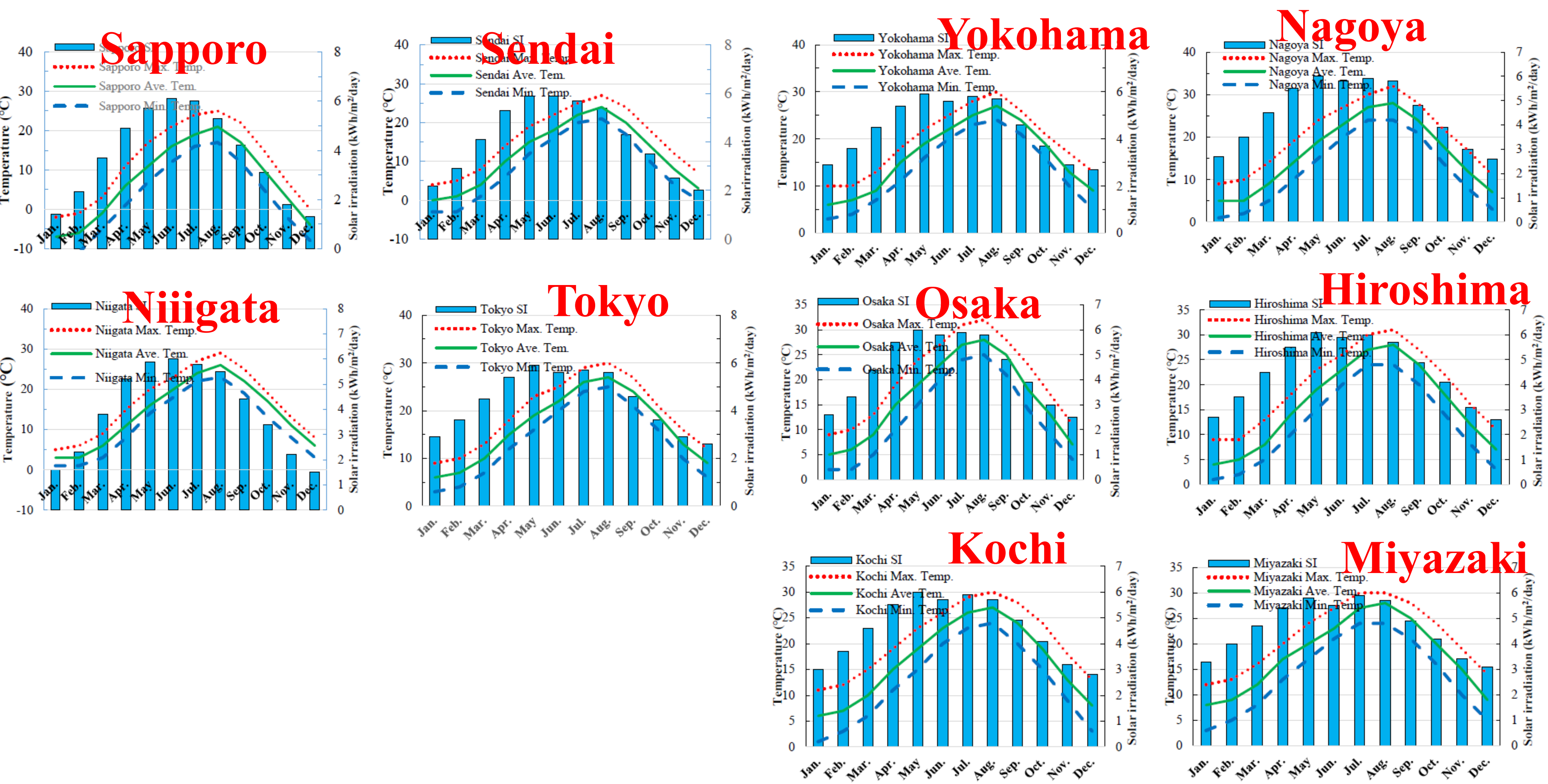

Daily average global solar irradiation [kWh/m^2/day] and monthly maximum, average and minimum ambient temperature [°C] in the major cities in Japan.

M. Yamaguchi et al., presented at the 40th EU-PVSEC Lisbon, Sep. 2023.

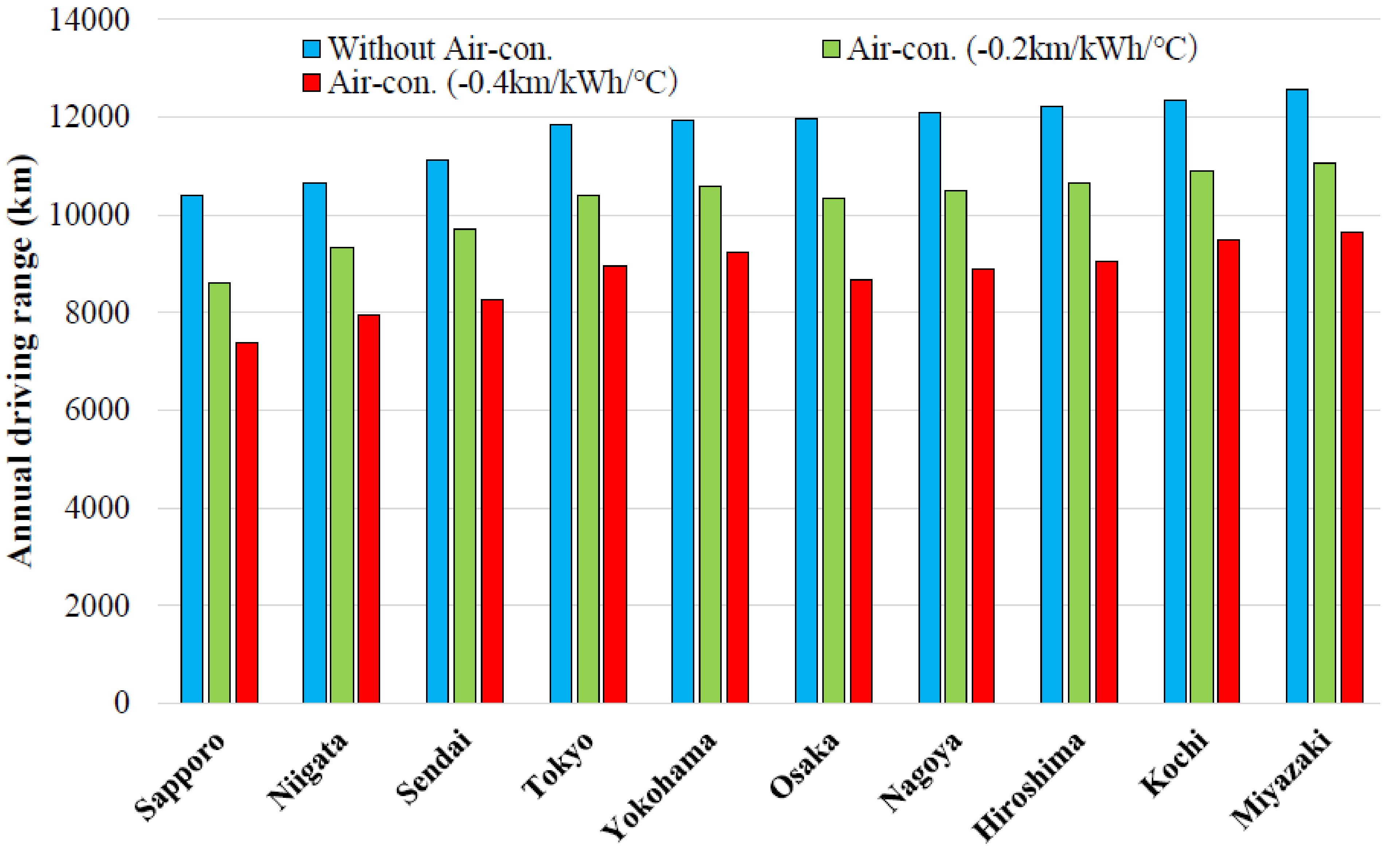

Annual driving distance calculated by considering power loss due to usage of air-conditioner for PV-EV installed with 1kW VIVP module and drove in major cities in Japan.

M. Yamaguchi et al., presented at the 40th EU-PVSEC Lisbon, Sep. 2023.

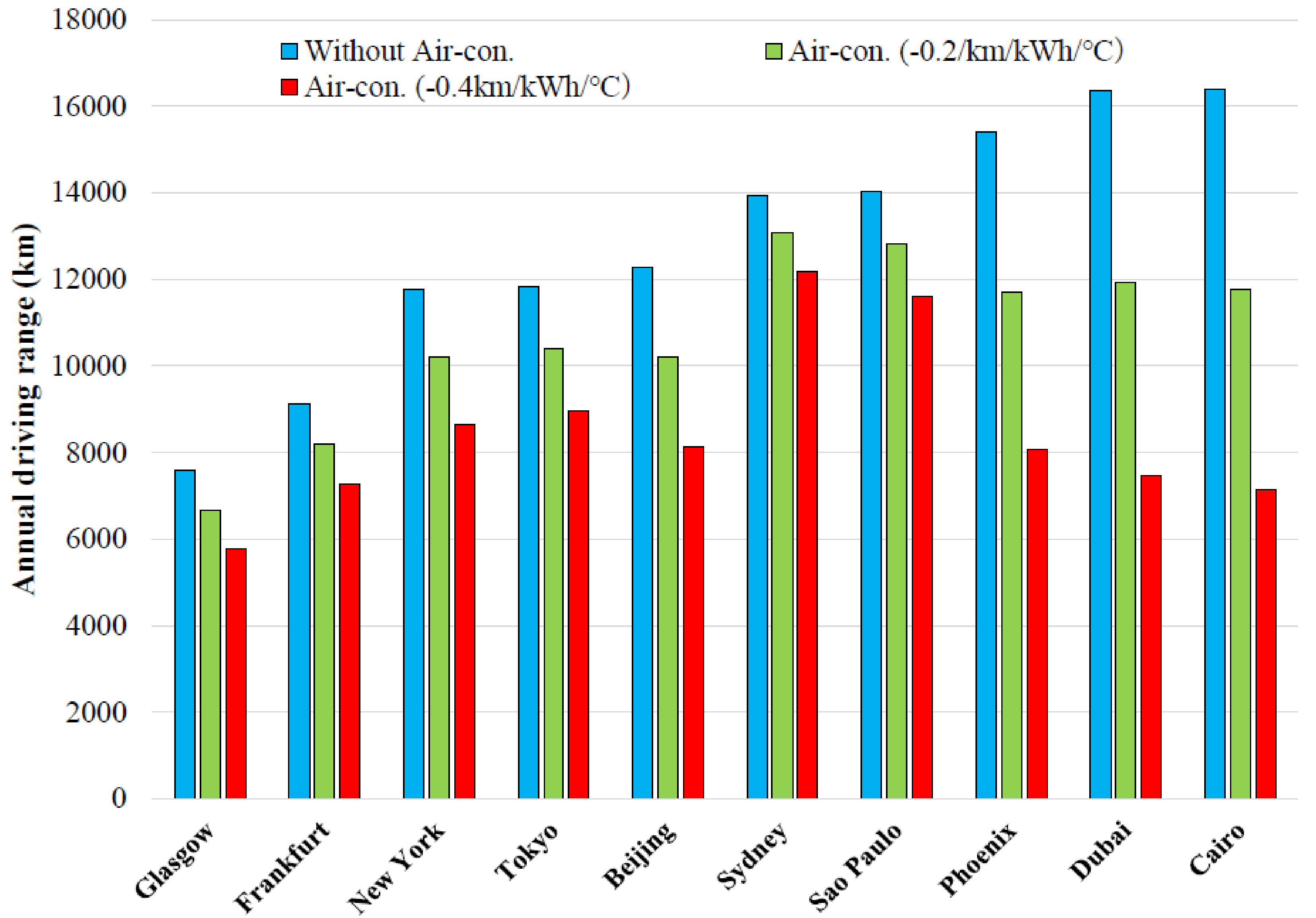

Annual driving distance calculated by considering power loss due to usage of air-conditioner for PV-EV installed with 1kW VIVP module and drove in major cities in the world.

M. Yamaguchi et al., presented at the 40th EU-PVSEC Lisbon, Sep. 2023.

Power loss analytical results of some factors for Toyota and Nissan demonstration cars.

	Usage of air-conditioner		Temperature rise		Partial shading		Estimated loss	Actual loss
	(-0.2km /kWh/°C)	(-0.4km /kWh/°C)	Yokohama	Nagoya	Araki et al. [ref. 28]	Hirota et al. [ref. 27]		
Toyota car		0.265		0.028	0.04	0.07	0.363	0.361
Nissan car	0.112		0.024		0.04	0.07	0.206	0.217

M. Yamaguchi et al., presented at the 40^{th} EU-PVSEC Lisbon, Sep. 2023.

3. High-efficiency and Low-cost Potential of Si Tandem Solar Cells

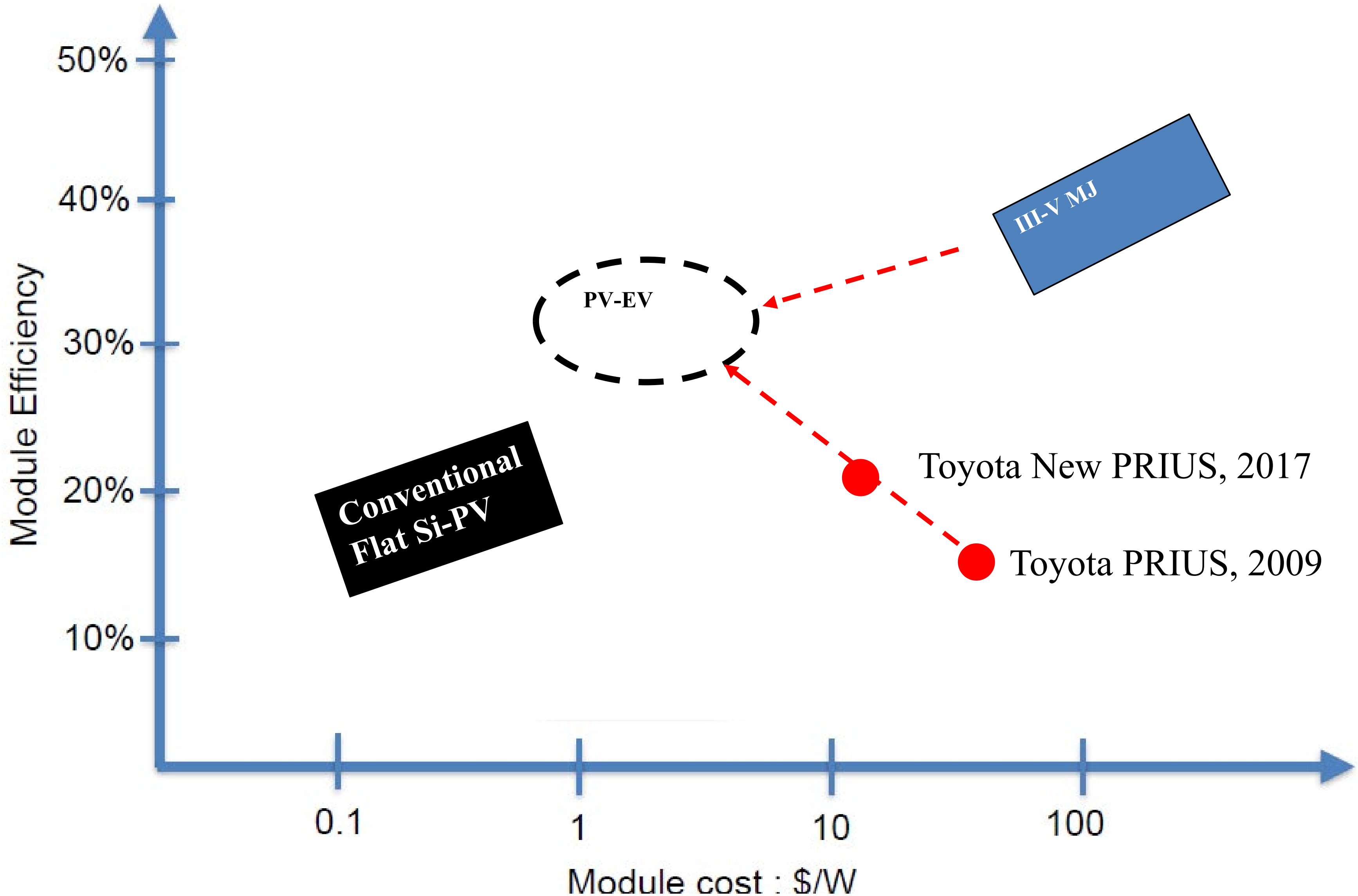

Module efficiency and module cost for III-V multi-junction solar cell modules, conventional flat Si PV solar cell modules, PV modules developed for Toyota Prius shipped in 2009, and those for Toyota New Prius shipped in 2017, and module efficiency and module cost targets of PV-EV.

M. Yamaguchi et al., Energy and Power Engineering **12**, 375 (2020).

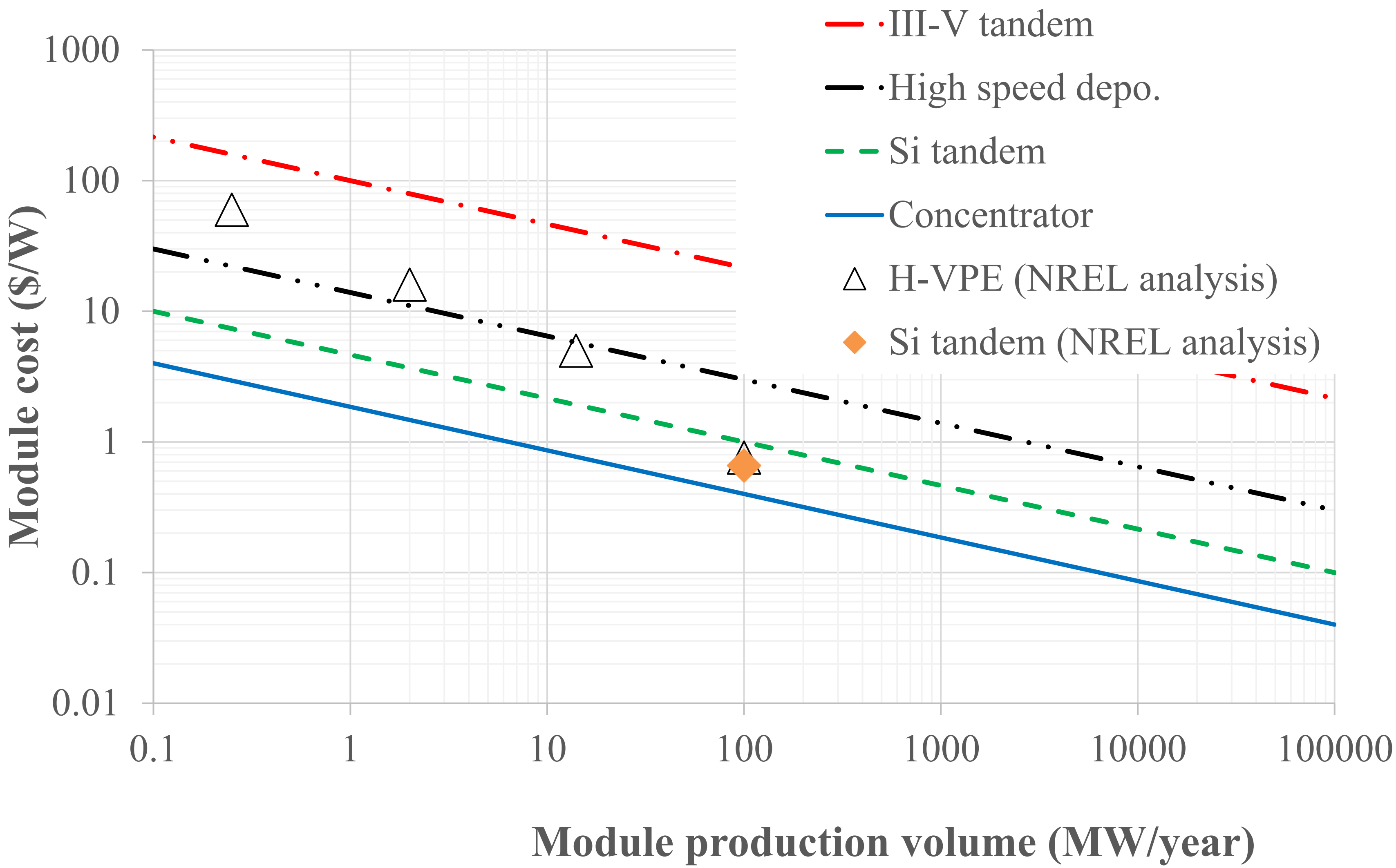

Comparison of module cost as a function of module production volume for a III-V tandem, high speed deposiion, Si tandem and concentrator solar cell modules reported by the authors in comparison with cost analytical results for high speed deposition and Si tandem reported by NREL.

M. Yamaguchi et al., Prog. Photovolt. DOI:10.1002/pip3343.

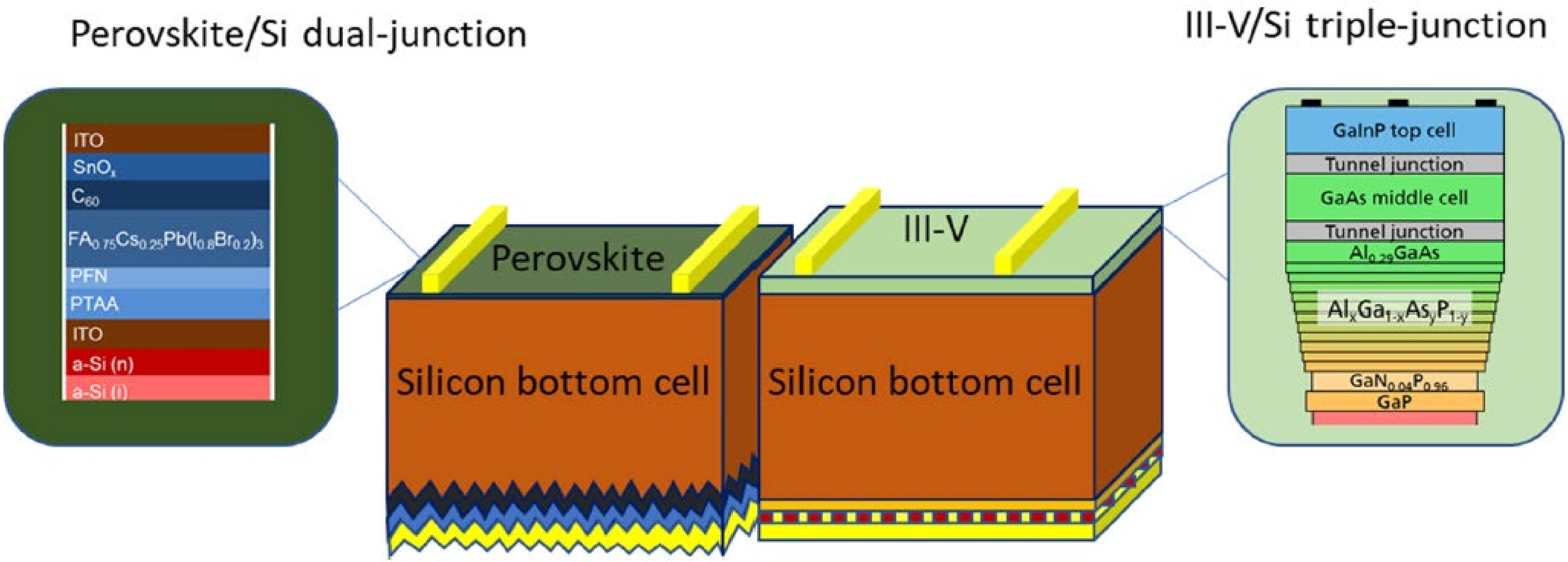

Examples for the layer structure of a perovskite/Si dual-junction solar cell structure with pyramids on the rear (left) and a GaInP/GaAs/Si triple-junction solar cell that uses a nanostructured resist grating as a diffusor on the back (right).

M. Yamaguchi et al., J. Appl. Phys. **129**, 240901 (2021).

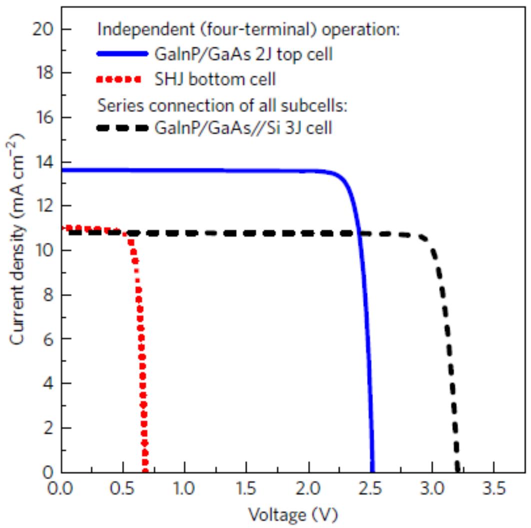

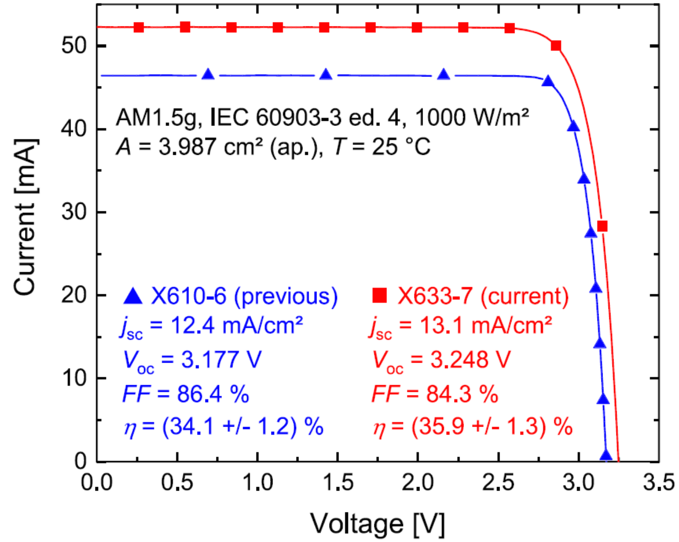

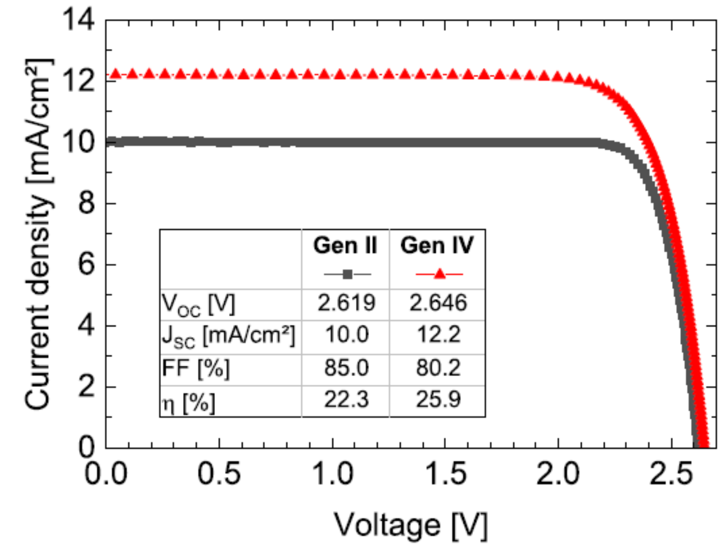

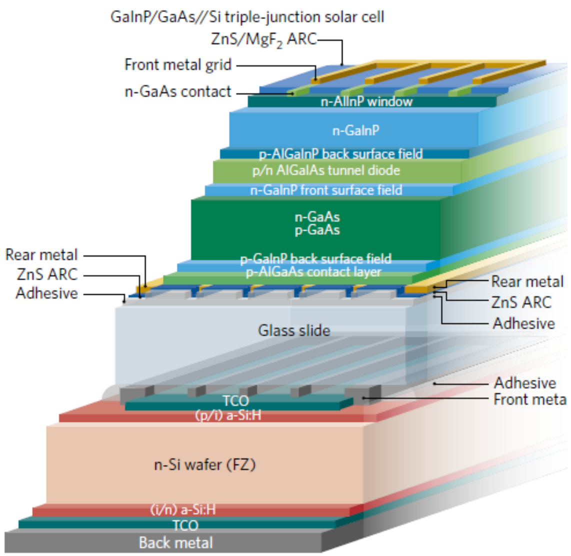

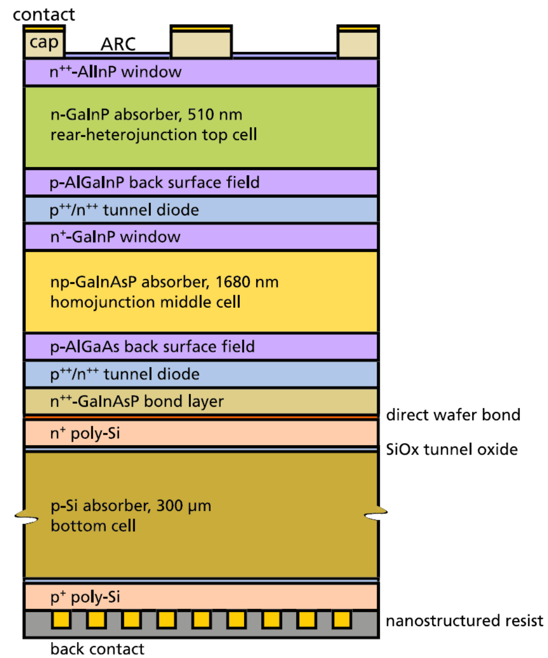

Mechnical Stact GaInP/GaAs /Si 3-J solar cell (35.9%)

S. Essig et al., Nature Energy **2,** 17144 (2017).

Wafer bonded GaInP/GaInAsP/Si 3-J solar cell (35.9%)

P. Schygulla et al., Prog. Photovolt. **30,** 869 (2022).

Direct-grown GaInP/GaAs /Si 3-J solar cell (25.9%)

M. Feifel et al., Solar RRL **5,** 2000763 (2021)

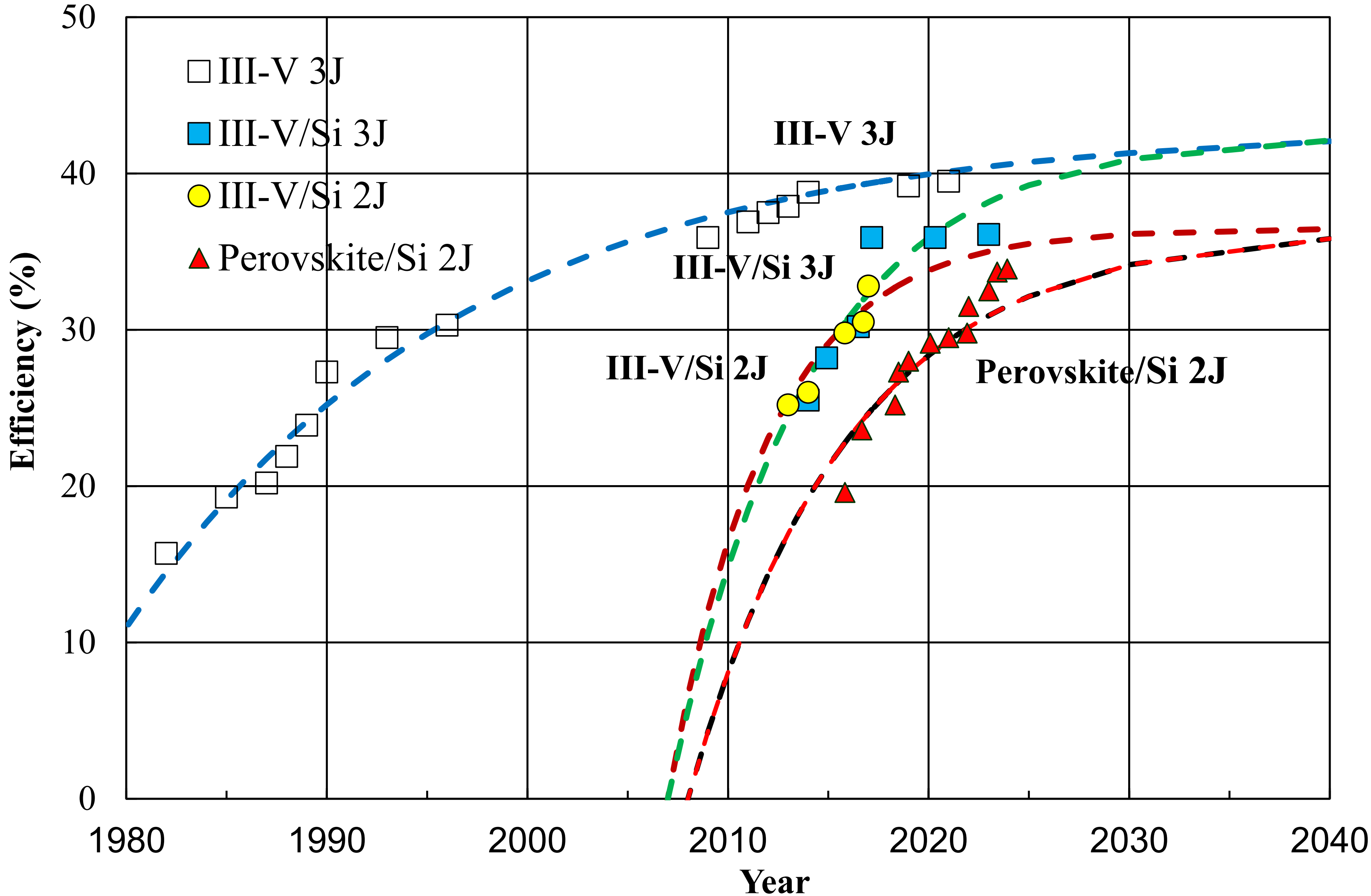

Chronological efficiency improvements of III-V/Si 3-junction, 2-junction and perovskite/Si 2-junction solar cells in comparison with those of III-V 3-junction solar cells under 1-sun condition.

M. Yamaguchi et al., Prog. Photovolt (2024). DOI: 10.1002/pip.3780.

Open-circuit voltage of solar cells is expreessed by

$V_{oc} = V_{oc:rad} + (kT/q)\ln(ERE)$, (9)

where k: Boltzmann constant, T: temperature, q: elementary charge.

$V_{oc:rad}$ is the radiative open-circuit voltage and we use $V_{oc;rad}$ valuesin our analysis:

Values of $E_g/q - V_{oc,\ rad}$ used are 0.23V for CIGS, CdTe, 0.26V for Si, 0.28V for III-V compounds and perovskite.

The second term on the right-hand side of eq. (9) is denoted as $V_{oc;nrad}$ because it associates to the voltage-loss due to non-radiative recombination.

In the case of multi-junction tandem solar cells, we define average ERE (ERE_{ave}) by using average Voc loss:

$\Sigma(V_{oc,n} - V_{oc,rad,n})/n = (kT/q)\ln(ERE_{ave})$, (10)

The resistance loss of a solar cell is estimated from the measured fill factor. The ideal fill factor FF_0, defined as the fill factor without any resistance loss, is estimated by

$FF_0 = (v_{oc} - \ln(v_{oc} + 0.71))/(v_{oc} + 1)$, (11)

where v_{oc} is $v_{oc} = V_{oc}/(nkT/q)$. (12)

The measured FF can be related to the series resistance and shunt resistance::

$FF \approx FF_0(1 - r_s)(1 - r_{sh}^{-1}) \approx FF_0(1 - r_s - r_{sh}^{-1}) = FF_0(1 - r)$, (13)

where r_s is the series resistance, and r_{sh} is the shunt resistance normalized to R_{CH}.

The characteristic resistance R_{CH} is defined by

$R_{CH} = V_{oc}/J_{sc}$, (14)

r is the total normalized resistance defined by $r = r_s + rsh^{-1.}$.

M. Yamaguchi et al., Progress in Photovoltaics 26, 543 (2018).

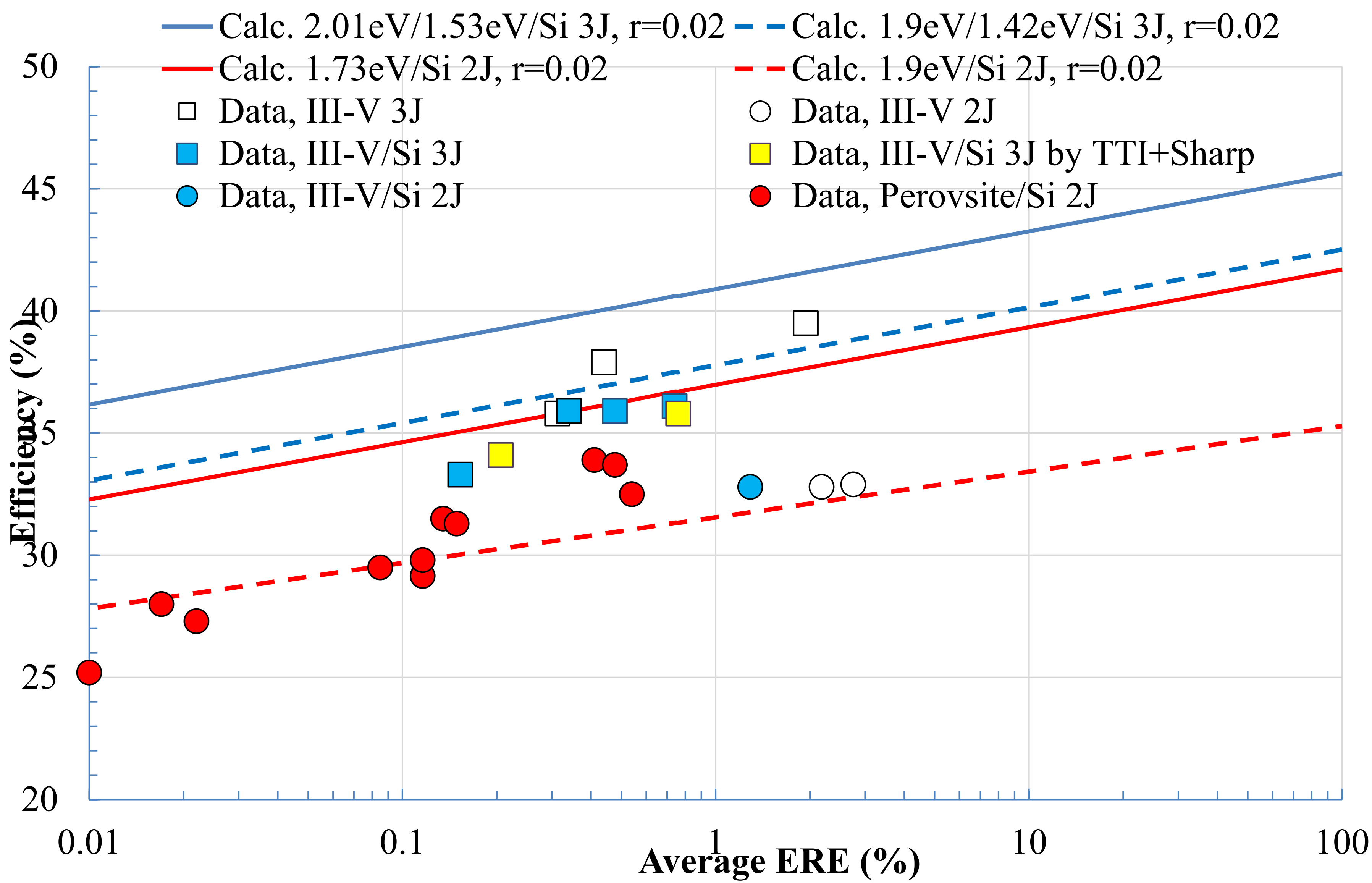

Calculated 1-sun efficiency of various Si tandem solar cells and III-V 3-junction solar cells including our results for III-/Si 3-junction tandem solar cells as a function of ERE and resistance loss $r_s + 1/r_{ss}$. White rectangular shows InGaP/GaAs/InGaAs triple-junction tandem solar cells.

M. Yamaguchi et al., Prog. Photovolt (2024). DOI: 10.1002/pip.3780.

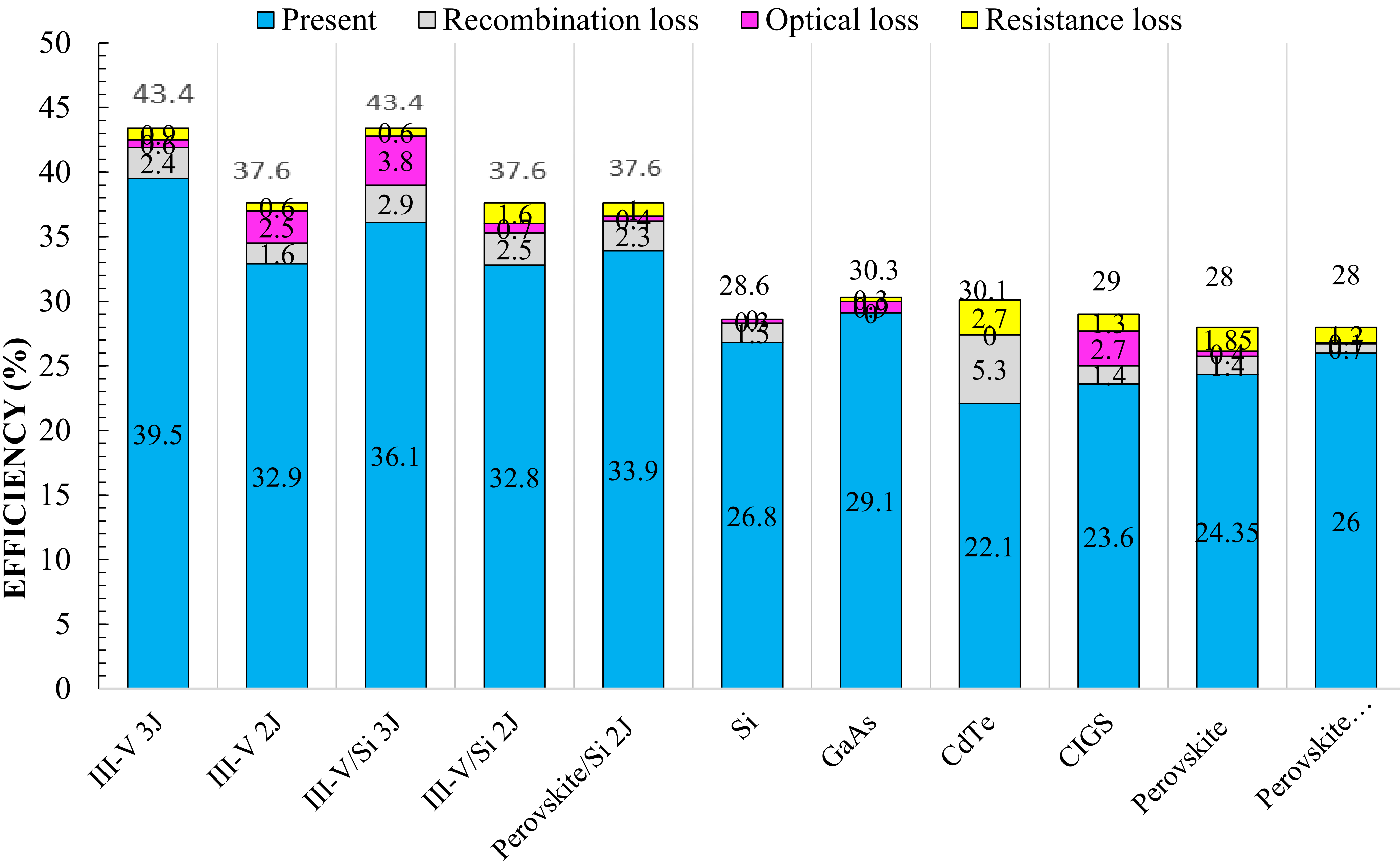

Analytical results for non-radiative recombination, optical and resistance losses of various Si tandem solar cells in comparison with those of single-junction and III-V 3-junction and 2-junction solar cells. M. Yamaguchi et al., Prog. Photovolt (2024). DOI: 10.1002/pip.3780.

豊田工業大学
TOYOTA TECHNOLOGICAL INSTITUTE

4. Our Recent Approaches on Si Tandem Solar Cells and Modules

Requirements of Solar Cell Modules for PV-powered Vehicles

- **High Performance**

  High efficiency

  Good temperature coefficient

  Good properties under low illumination intensity
- **Low Cost**
- **3 Dimensional Curvature**
- **Color Variation**

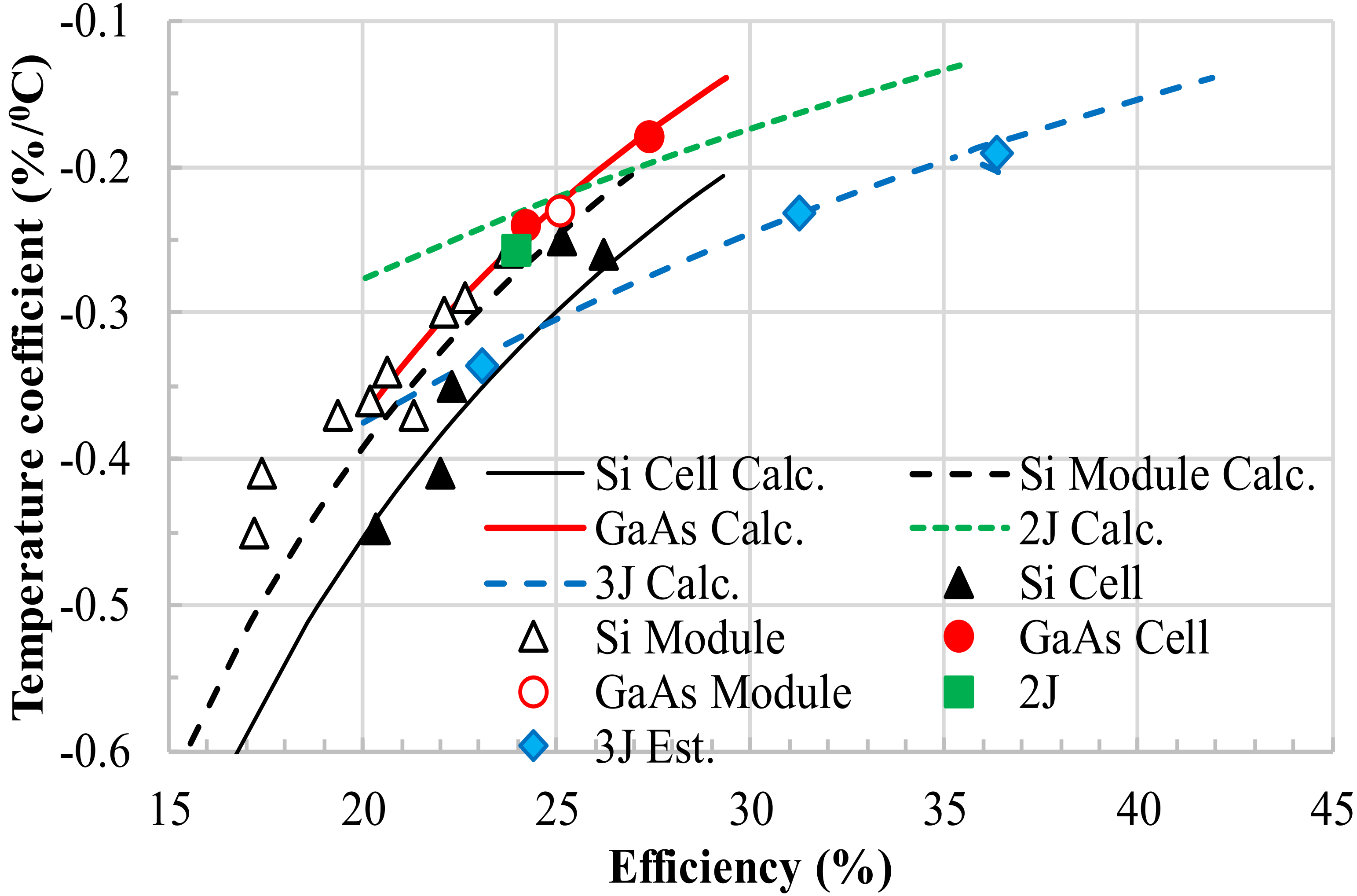

Calculated results for temperature coefficients of crystalline Si, GaAs and III-V compound triple-junction cells and modules as a function of its conversion efficiencies of the cells and modules in comparison with reported values and estimated values..

M. Yamaguchi et al., J. Phys. D: Appl. Phys. 54, 504002 (2021).

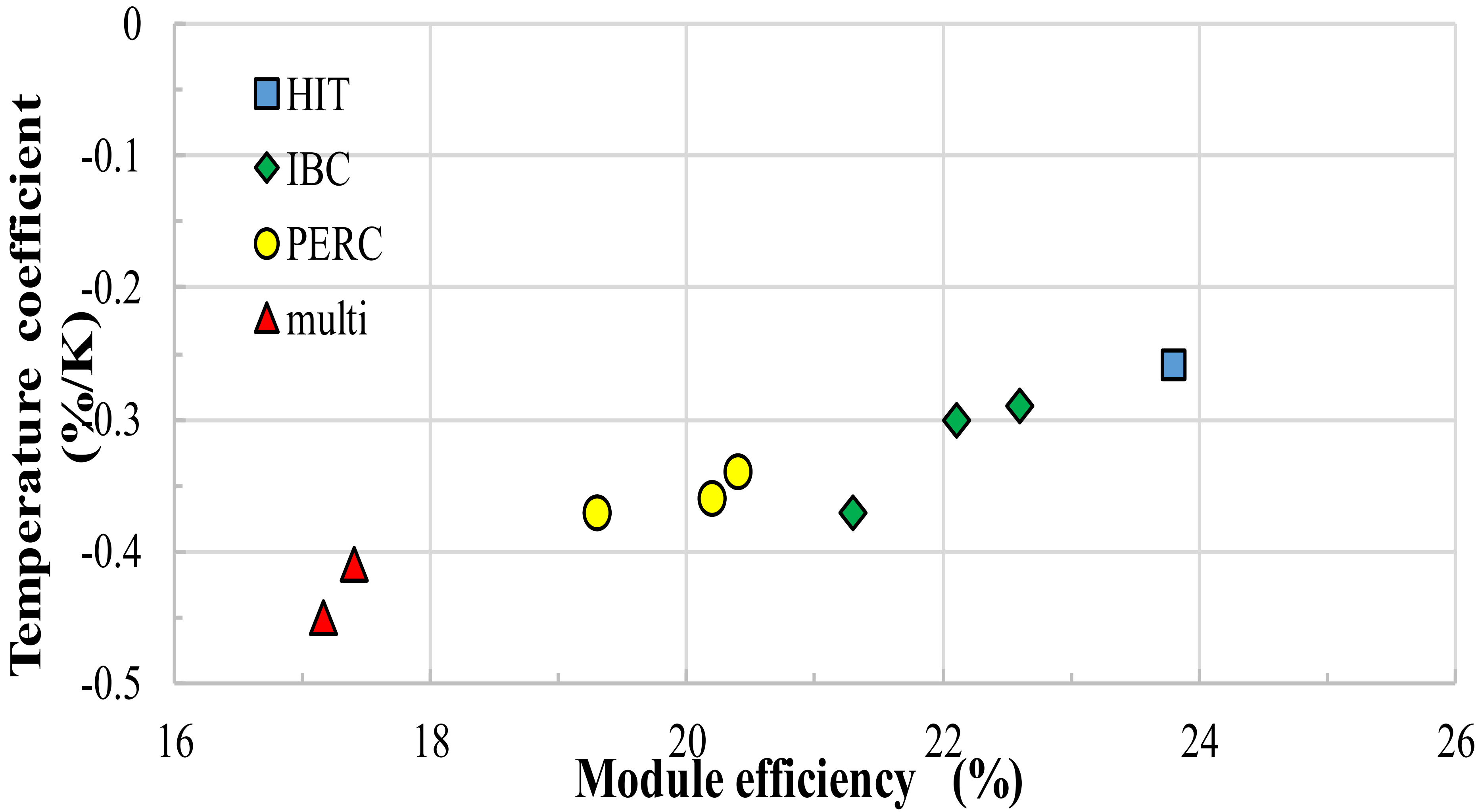

Reported values temperature coefficients of crystalline Si solar cell modules as a function of module efficiency.

M. Yamaguchi et al., J. Phys. D: Appl. Phys. 54, 504002 (2021).

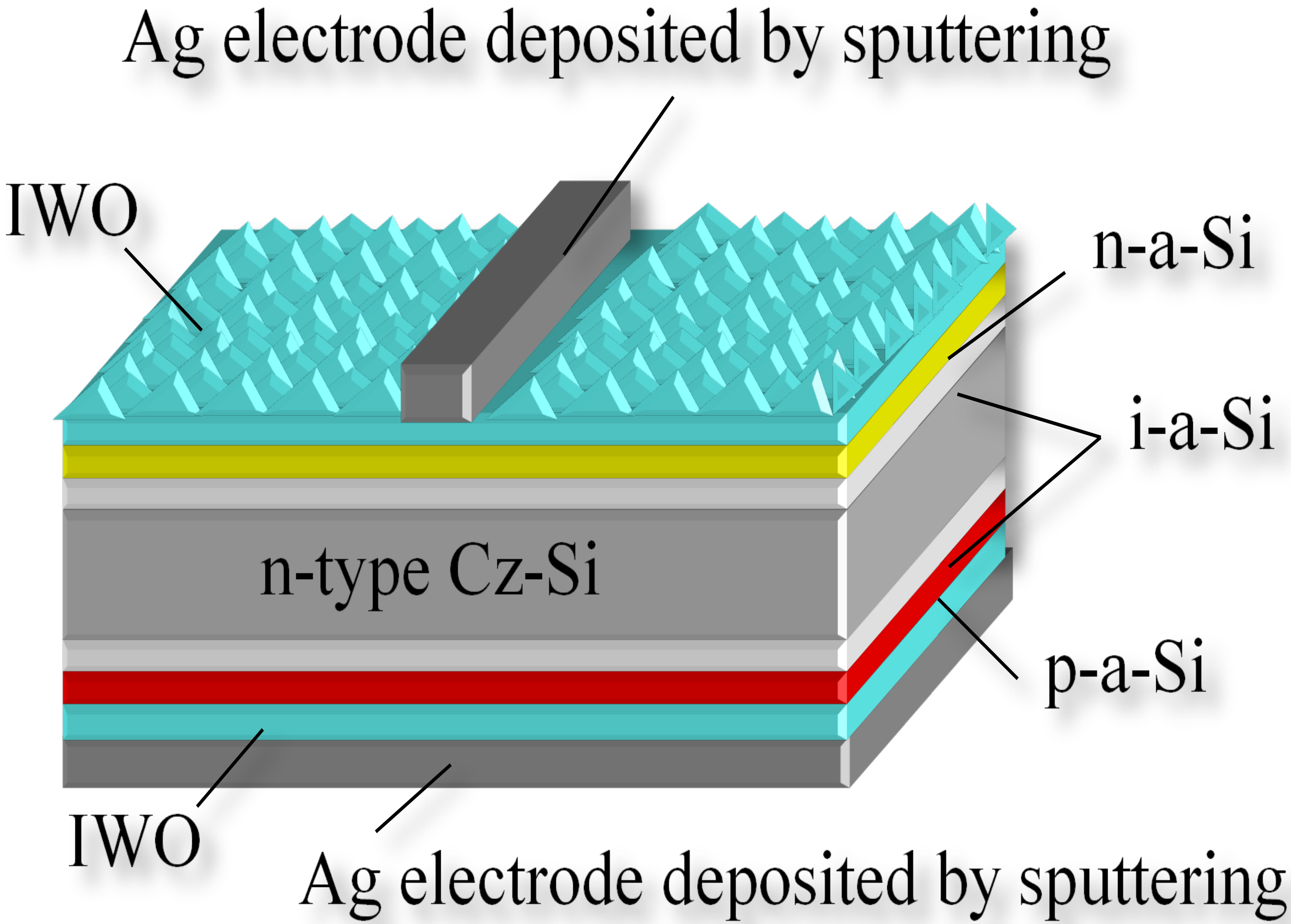

A structure of Si heterojunction solar cell fabricated.

M. Yamaguchi et al., presented at the 40th EU-PVSEC, Lisbon, Sep. 18-22, 2023

	Jsc [mA/cm²]	Voc [V]	FF	η [%]
TTI SHJ (48mm x 48mm)	40.13	0.729	0.85	24.88

	Voc (V)	Jsc (mA/cm2)	FF	Cell efficiency (%)	Tandem cell efficiency (%)
InGaP/GaAs 2J top cell	2.546	13.81	0.860	30.23	35.81
Si bottom cell	0.691	9.96	0.811	5.58	

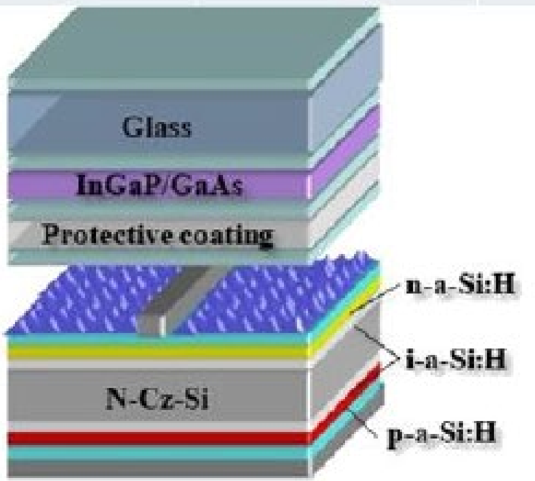

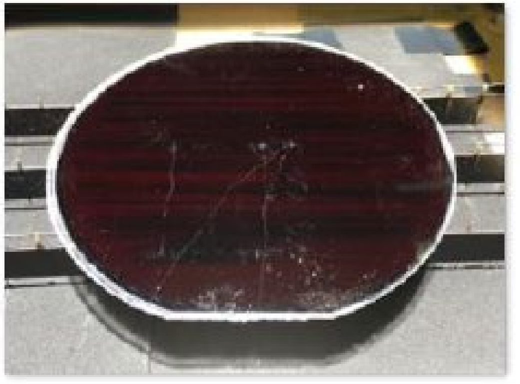

A structure, photo and roperties of Si hetero-junction solar cell and 4-terminal InGaP/GaAs/Si 3-junction solar cell.

M. Yamaguchi et al., Prog. Photovolt (2024). DOI: 10.1002/pip.3780.

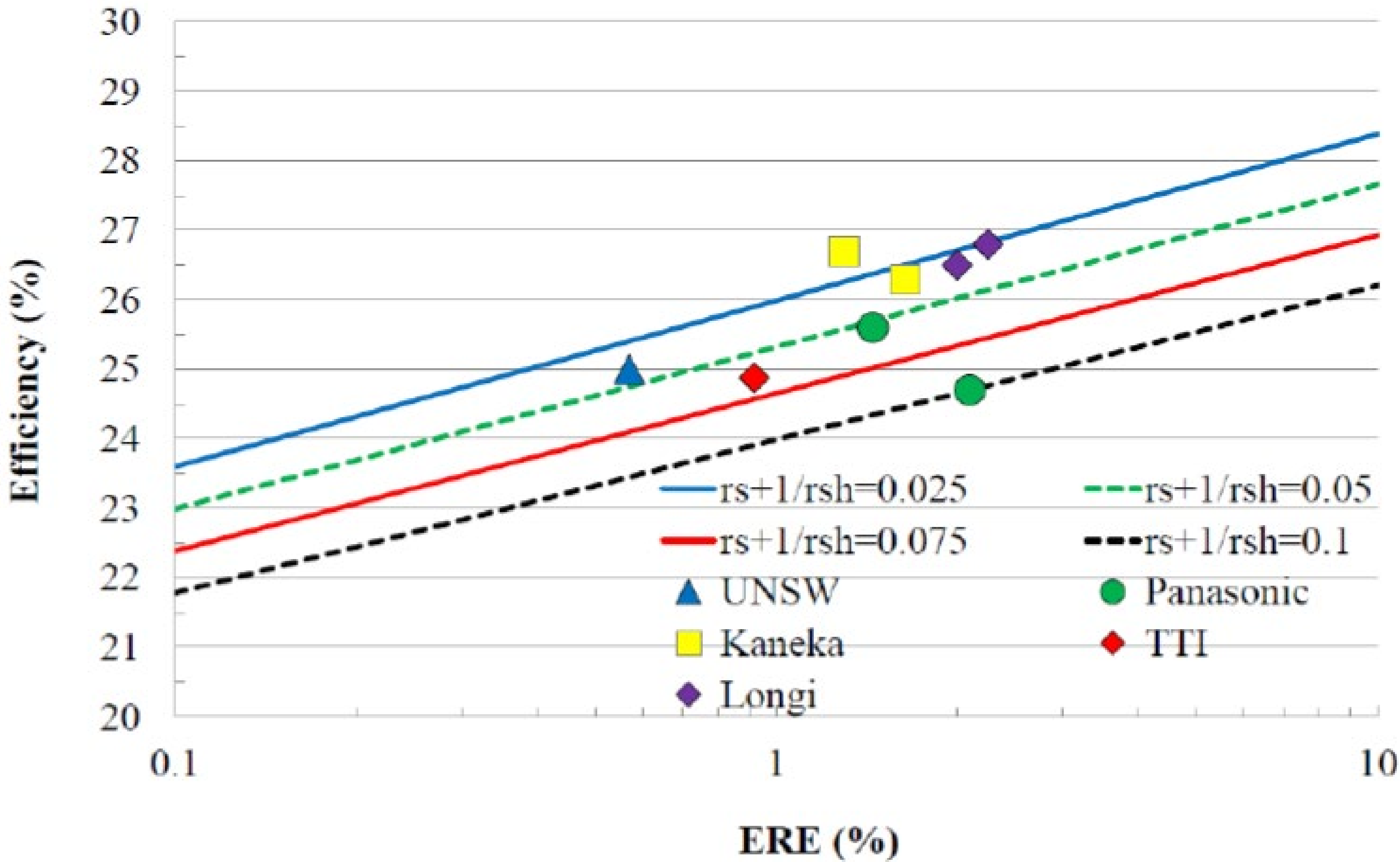

Calculated efficiencies of crystalline Si solar cells as a function of external radiative efficiency (ERE) in comparison with realized efficiencies of Si solar cells reported by UNSW, Panasonic, Kaneka, Longi and authors (TTI).

M. Yamaguchi et al., Prog. Photovolt (2024). DOI: 10.1002/pip.3780.

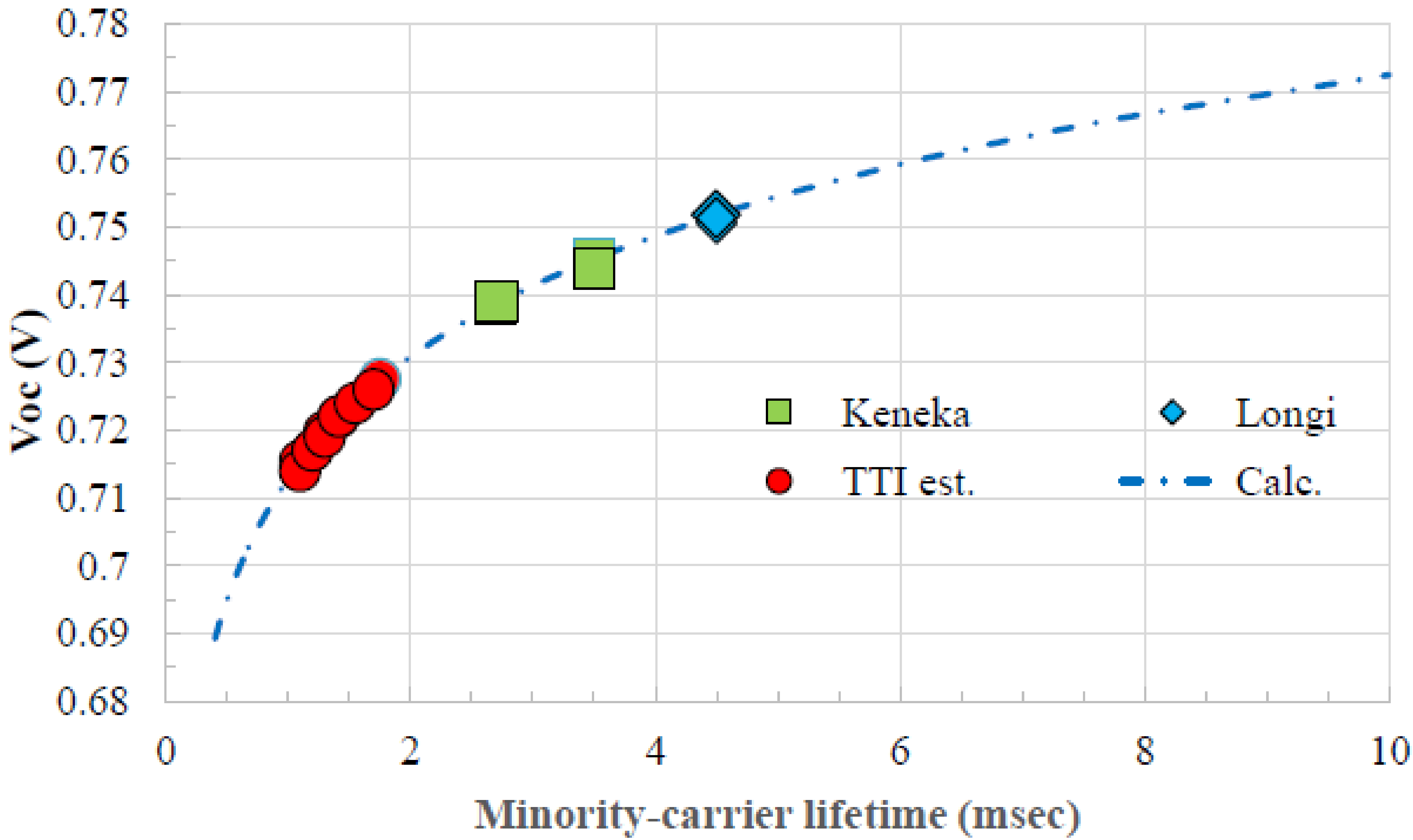

Changes in open-circuit voltage Voc of SHJ solar cells by Kaneka, Longi and the authors as a function of minority-carrier lifetime.

M. Yamaguchi et al., Prog. Photovolt (2024). DOI: 10.1002/pip.3780.

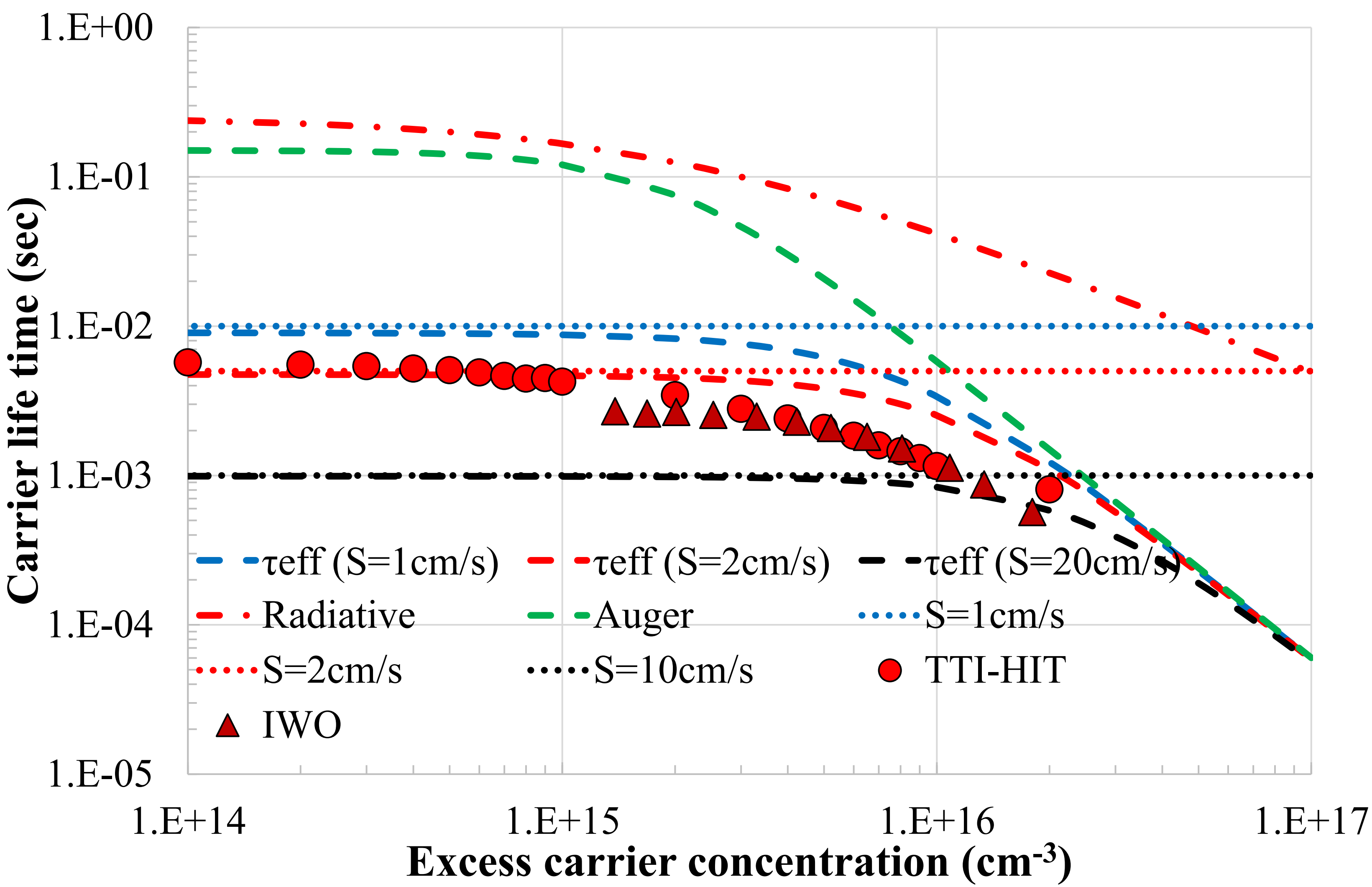

Comparison of the measured and simulated minority carrier lifetimes as a functions of excess carrier density for our two cases after surface passivation and IWO deposition.

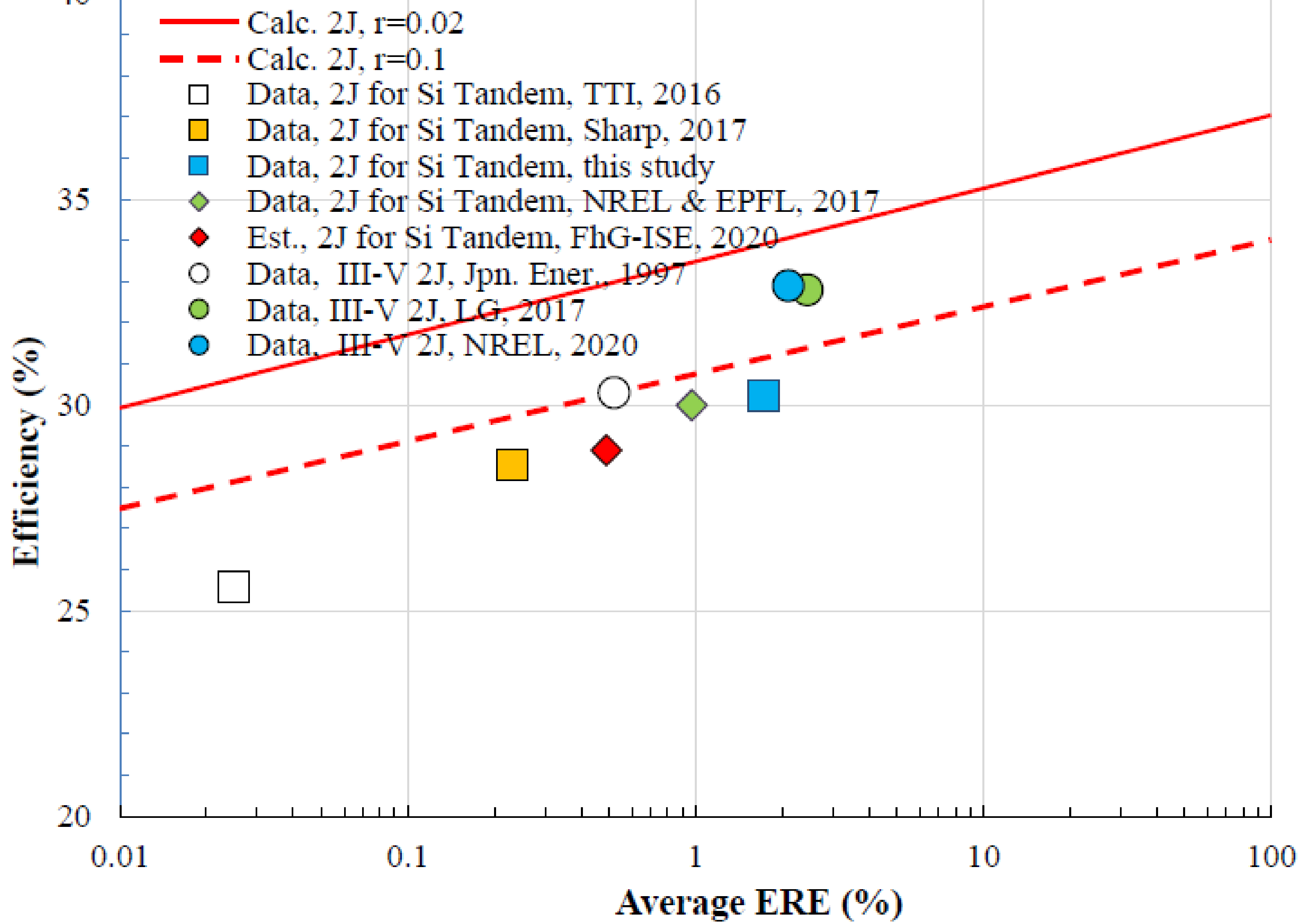

Calculated efficiencies of III-V 2-junction solar cells as a function of external radiative efficiency (ERE) in comparison with realized efficiencies of III-V 2-junction uper solar cells for III-V/Si 3-junction tandem solar cells reported by the authors, Sharp including this study, NREL& EPFL and FhG-ISE in compairson with those of III-V 2-junction solar cells reported by LG and NREL.

M. Yamaguchi et al., presented at the 40th EU-PVSEC, Lisbon, Sep. 18-22, 2023

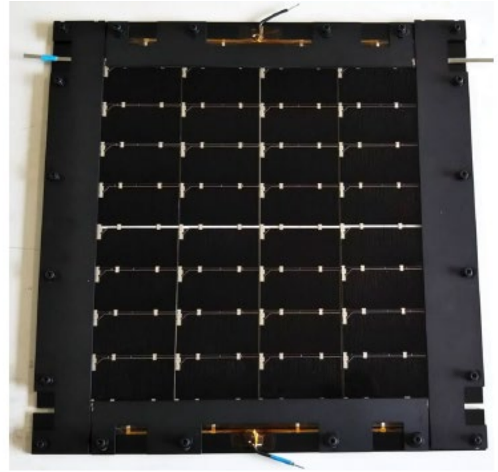

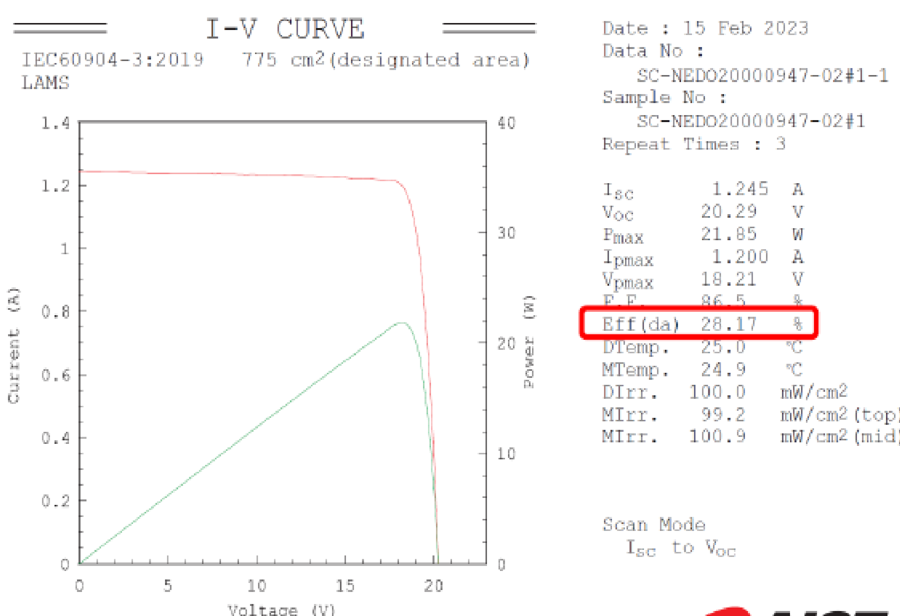

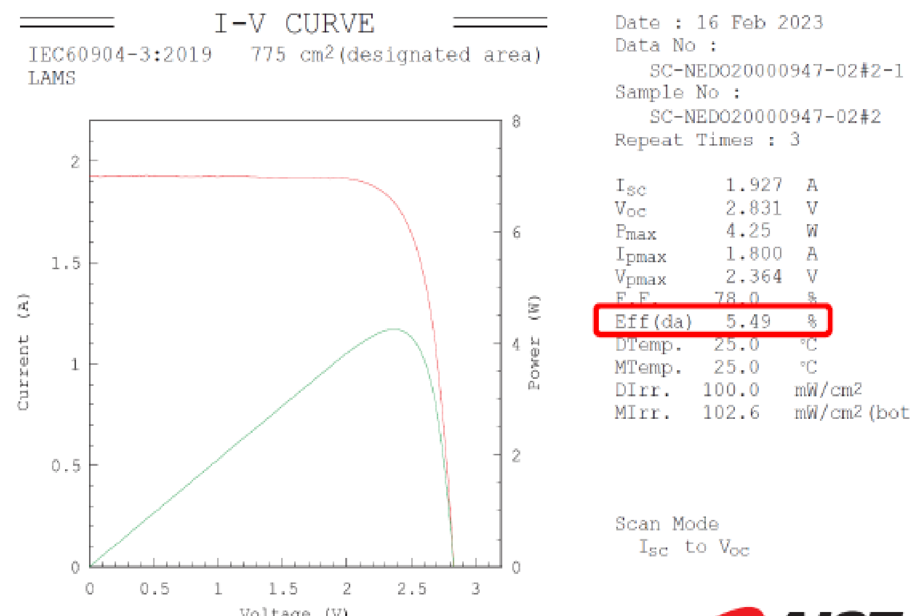

A photo of new record efficiency InGaP/GaAs/Si 3-junction solr cell module and I–V charactersitics of InGaP/GaAs upper 2-junction solar cell module and Si bottom solar cell module.

M. Yamaguchi et al., presented at the 40th EU-PVSEC, Lisbon, Sep. 18-22, 2023

The characteristic solar cell module parameters confirmed by the AIST.

	Area (cm^2)	Isc (A)	Voc (V)	FF (%)	Pm (W)	Module Efficiency (%)	Tandem Cell Module Efficiency (%)
InGaP/GaAs 2J top cell module	775	1.245	20.29	86.5	21.85	28.17	33.66
Si bottom cell module	775	1.927	2.831	73.0	4.25	5.49	

M. Yamaguchi et al., Prog. Photovolt (2024). DOI: 10.1002/pip.3780.

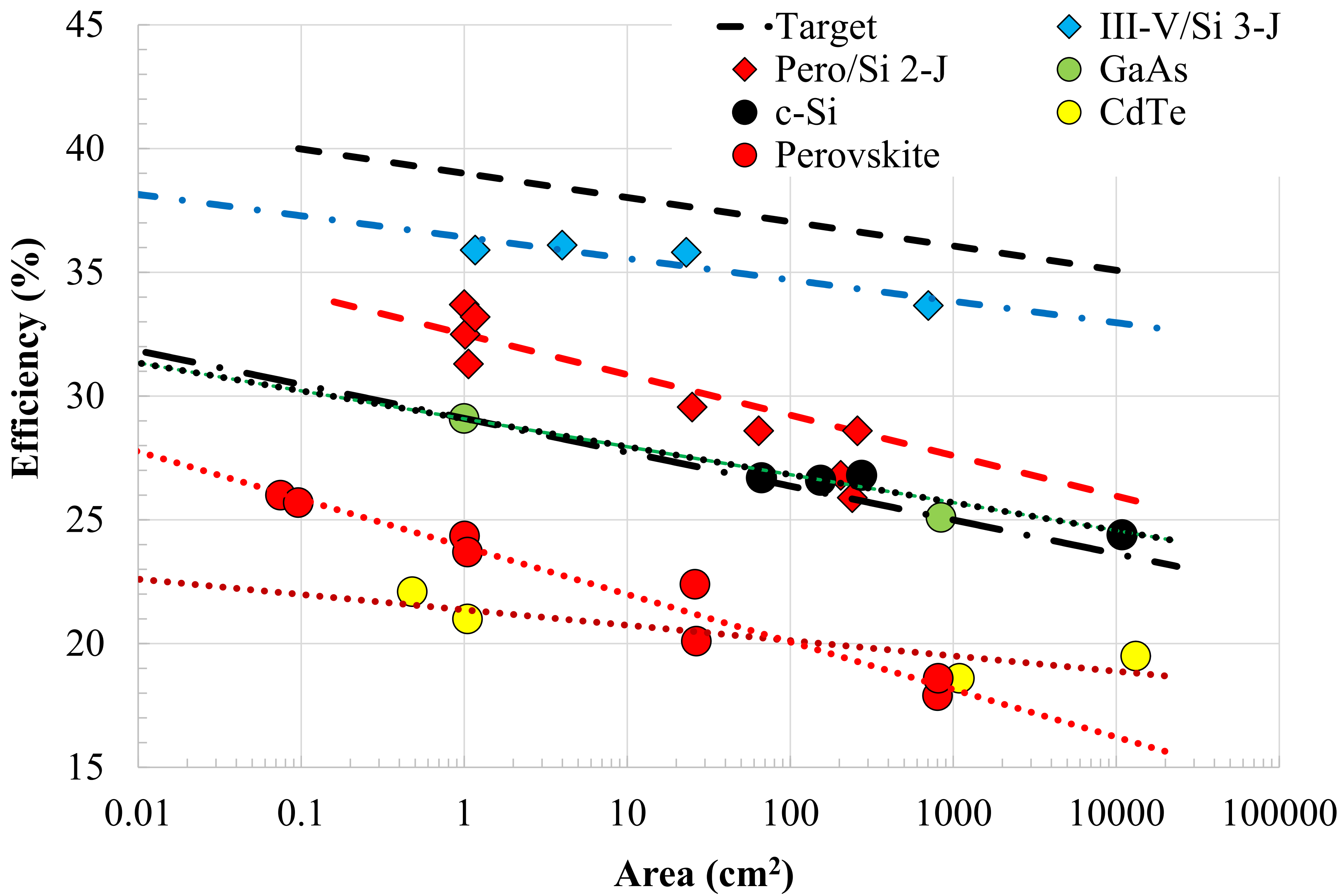

Changes in conversion efficiency of Si, GaAs, CdTe, perovskite single-junction solar cells and modules, and III-V/Si 3-junction and perovskite/Si 2-junction tandem solar cell and modules versus area of solar cells and modules.

M. Yamaguchi et al., Prog. Photovolt (2024). DOI: 10.1002/pip.3780.

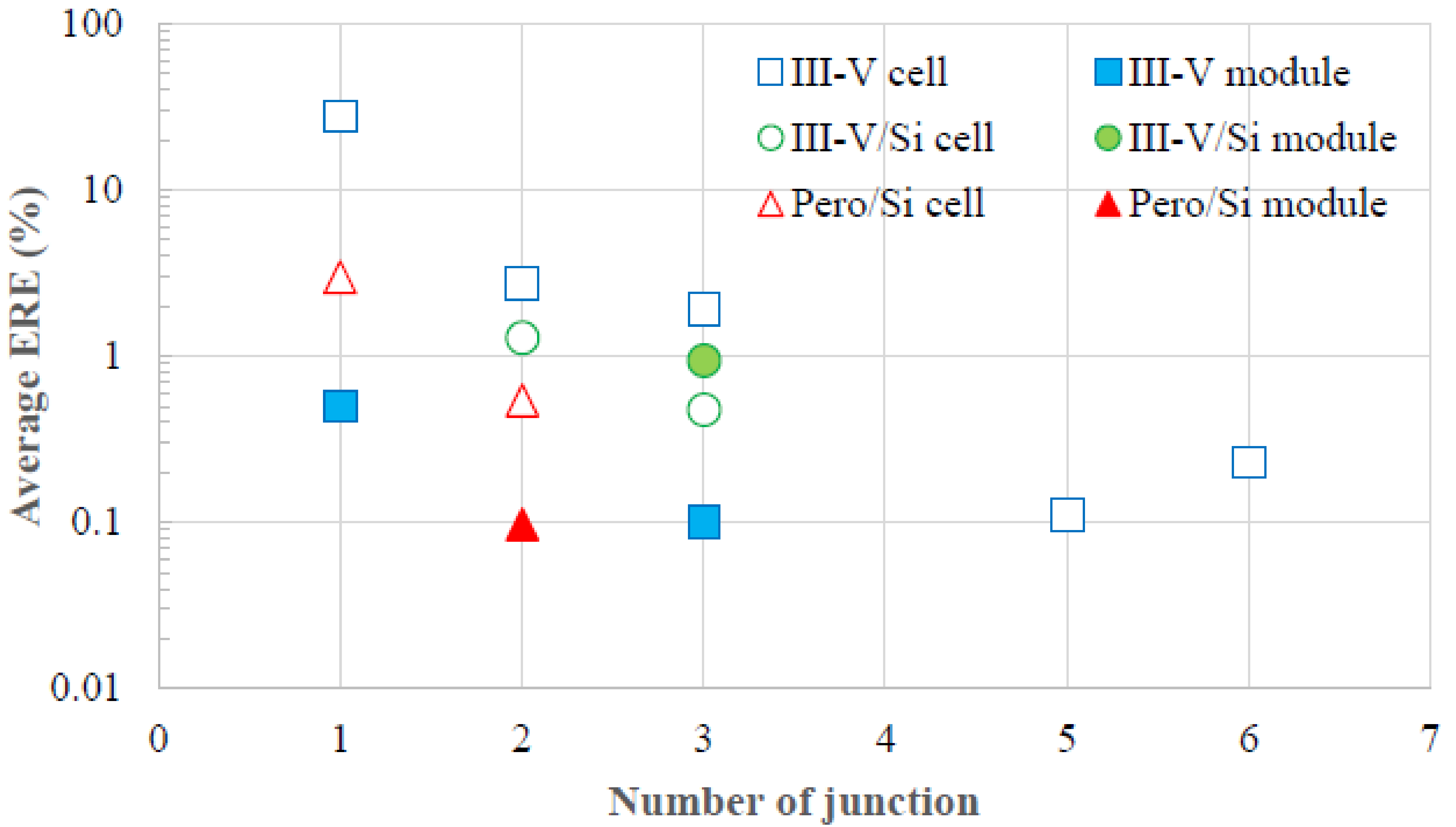

Changes in average external radiative efficiency ERE for III-V multi-junction, III- V/Si tandem and perovskite/Si tandem solar cells and modules as a function of number of junctions.

M. Yamaguchi et al., presented at the 40th EU-PVSEC, Lisbon, Sep. 18-22, 2023

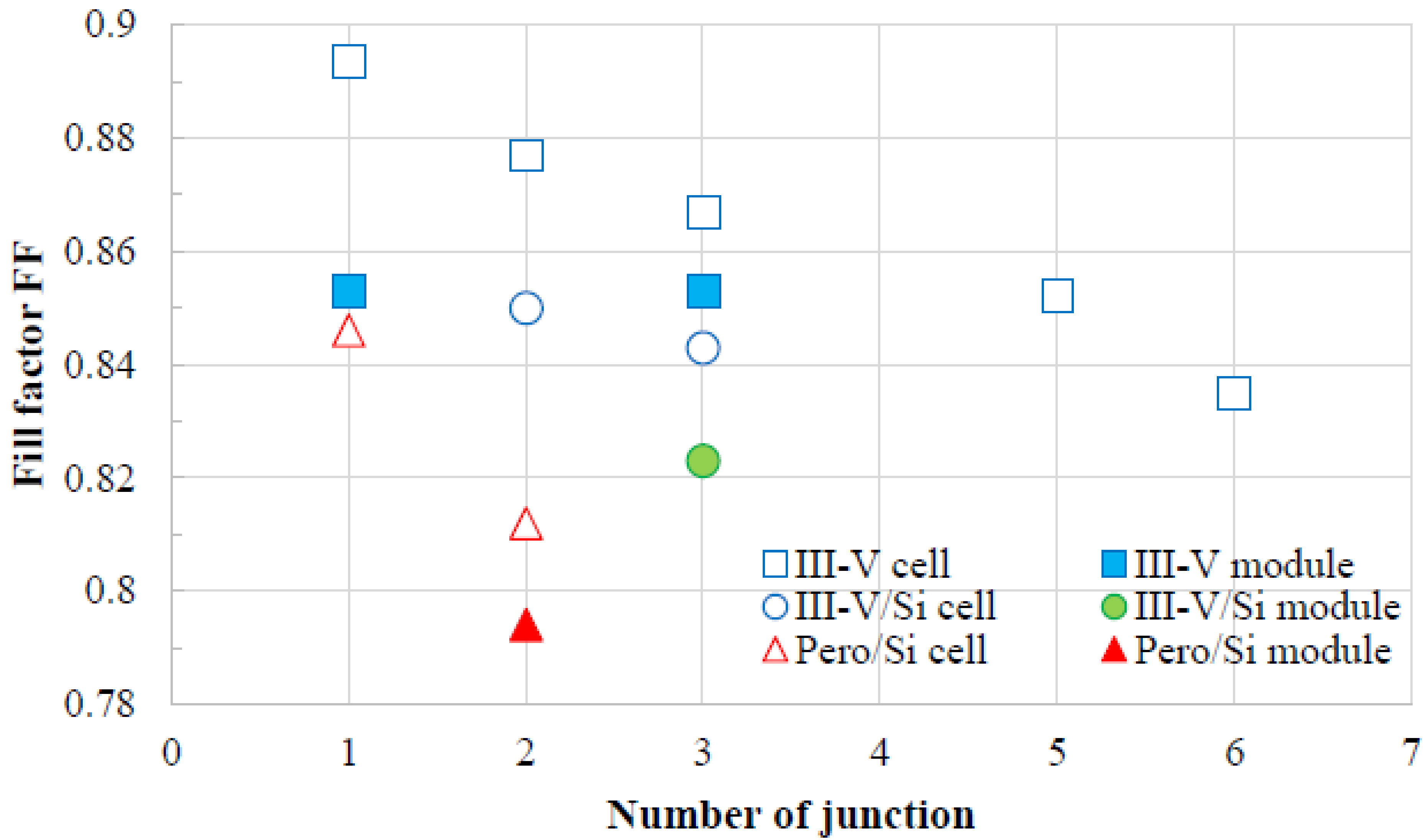

Changes in fill FF for III-V multi-junction, III-V/Si tandem and perovskite/Si tandem solar cells and modules as a function of number of junctions.

M. Yamaguchi et al., presented at the 40th EU-PVSEC, Lisbon, Sep. 18-22, 2023

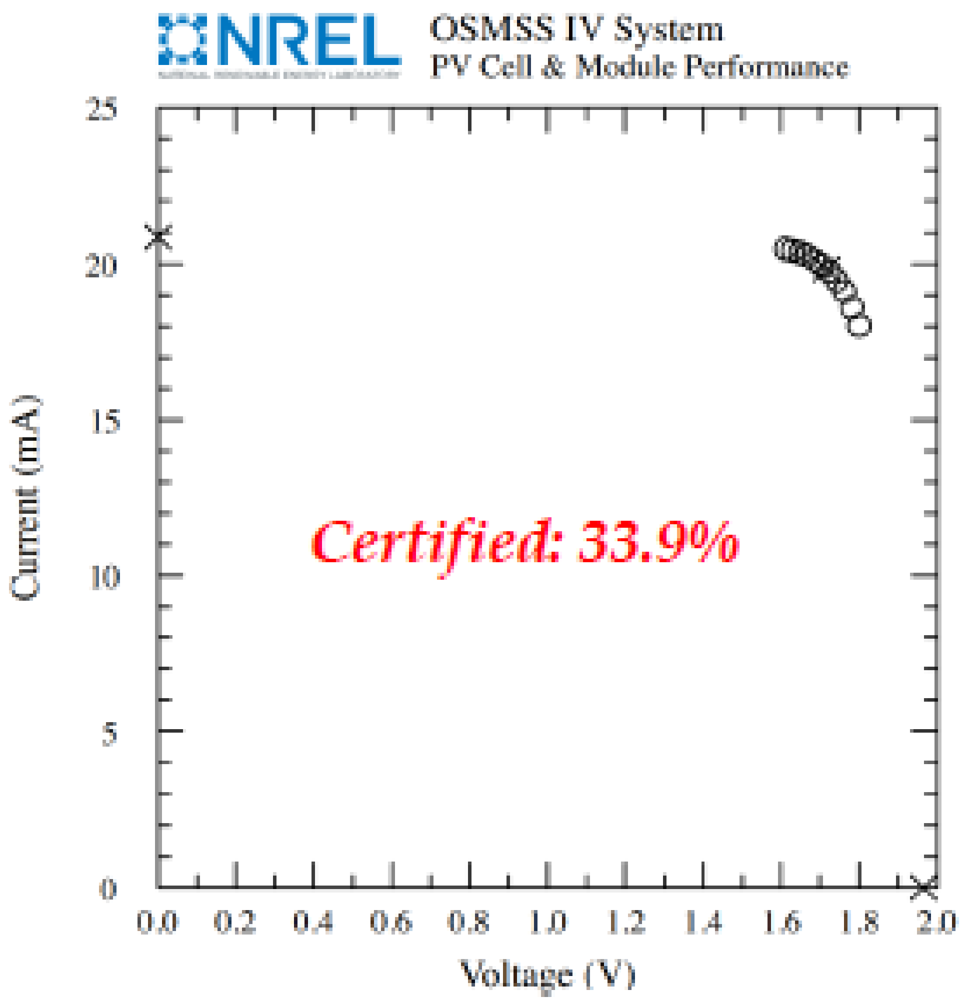

V_{oc} = 1.9657 V ± 0.84%
I_{sc} = 20.852 mA ± 0.52%
J_{sc} = 20.761 mA/cm^2 ± 0.64%
Fill Factor = (83.0 ± 1.14)%
I_{max} = 19.826 mA ± 0.54%
V_{max} = 1.7168 V ± 0.78%
P_{max} = 34.037 mW ± 0.87%
Efficiency = (33.89 ± 0.29)%

New record efficiency (33.9%) perovskite/Si 2-junction tandem solar cell by Longi.

(J. Liu et al., PVSEC-34, Shenzhen, China, Nov. 6-10, 2023)

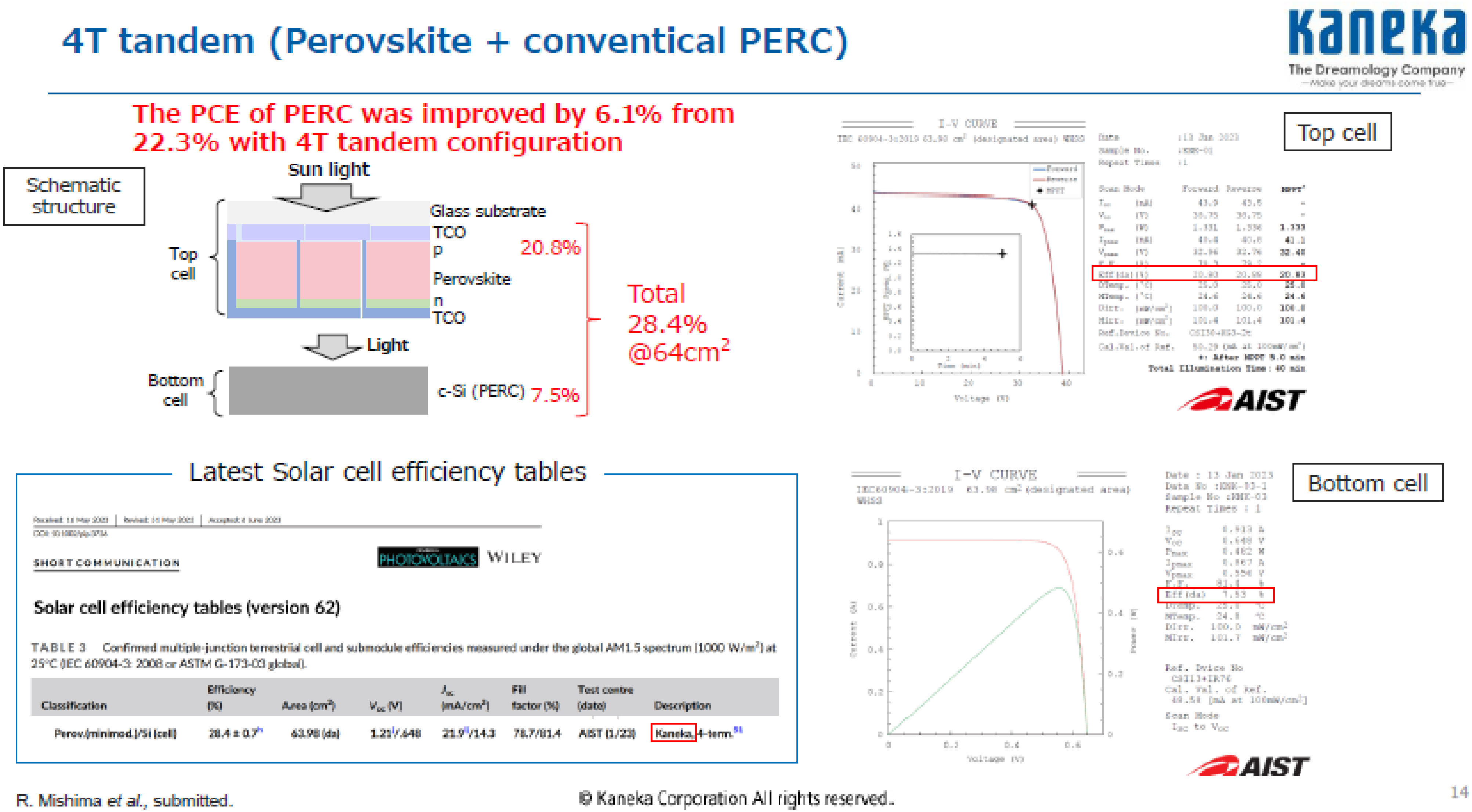

4T perovskite/Si-PERC 2-junction tandem solar cell (certified: 28.5% @64 cm^2) and perovskite/Si-HBC 2-junction tandem solar cell (in-house measurement: 30.8% @64 cm^2) by Kaneka.

(M. Kanematsu et al., PVSEC-34, Shenzhen, China, Nov. 6-10, 2023)

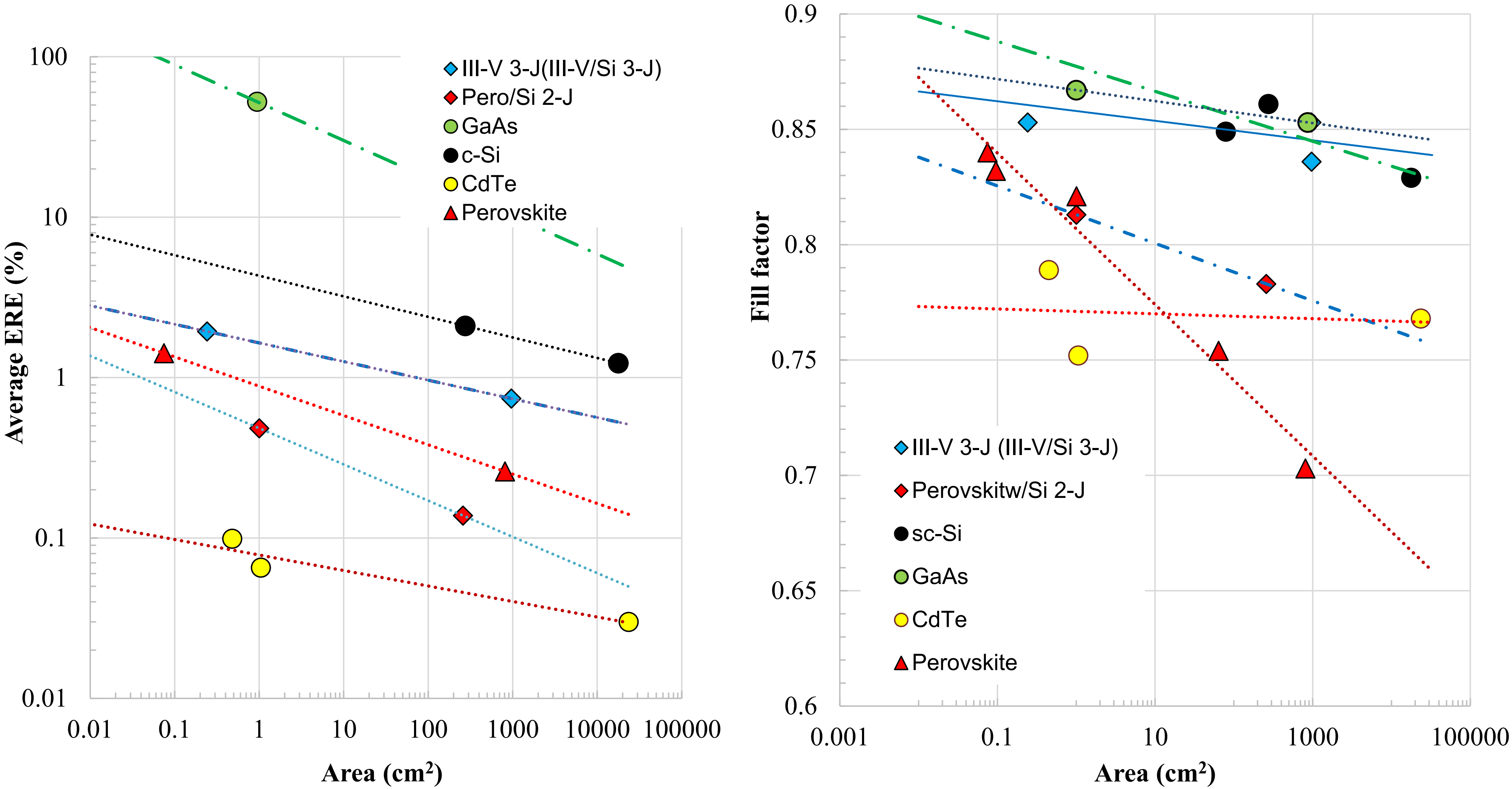

Changes in average ERE (external radiative efficiency) and fill factor of Si, GaAs, CdTe, perovskite single-junction solar cells and modules, and III-V/Si 3-junction and perovskite/Si 2-junction tandem solar cell and modules versus area of solar cells and modules.

Summary

This paper presented effectiveness of high-efficiency solar cell modules from point-views of driving distance, reduction in CO_2 emission with 55-70 % reduction and saving EV charging cost with $170-250/year.

The Si tandem solar cells are expected to have significant potential for PV-powered vehicle applications because of high efficiency with efficiencies of more than 42% under 1-sun AM1.5 G, lightweight and low-cost potential.

Most recently, the authors have achieved 35.8% efficiency with InGaP/GaAs/Si 3-junction tandem solar cell (area of 23 cm^2) and new record efficiency 33.7% with 3-junction tandem solar cell module (area of 775 cm^2).

It is summarized that the III-V/Si 3-junction solar cell modules have potential of driving distance of more than 30 km/day average and more than 50 km/day on a clear day.

豊田工業大学
TOYOTA TECHNOLOGICAL INSTITUTE

Si Tandem Solar Cells

IOP Publishing | Journal of Physics D: Applied Physics

J. Phys. D: Appl. Phys. **51** (2018) 133002 (13pp) | https://doi.org/10.1088/1361-6463/aaaf08

Topical Review

A review of recent progress in heterogeneous silicon tandem solar cells

Masafumi Yamaguchi, Kan-Hua Lee[1], Kenji Araki and Nobuaki Kojima

Toyota Technological Institute, Hisakata 2-12-1, Tempaku-ku, Nagoya, Japan

豊田工業大学
TOYOTA TECHNOLOGICAL INSTITUTE

Multi-junction Solar Cells

Journal of Applied Physics

PERSPECTIVE

scitation.org/journal/jap

Multi-junction solar cells paving the way for super high-efficiency

Cite as: J. Appl. Phys. **129**, 240901 (2021); doi: 10.1063/5.0048653
Submitted: 25 February 2021 · Accepted: 1 June 2021 ·
Published Online: 23 June 2021

View Online Export Citation CrossMark

Masafumi Yamaguchi,[1,a)] Frank Dimroth,[2] John F. Geisz,[3] and Nicholas J. Ekins-Daukes[4]

AFFILIATIONS

[1]Toyota Technological Institute, Nagoya 468-8511, Japan
[2]Fraunhofer Institute for Solar Energy Systems ISE, Freiburg 79110, Germany
[3]National Renewable Energy Laboratory, Golden, Colorado 80401, USA
[4]School of Photovoltaic & Renewable Energy Engineering, University of New South Wales, Sydney 2052, Australia


Be Ambitious for Your Dreams
and Your Wishes!
Thank you very much!

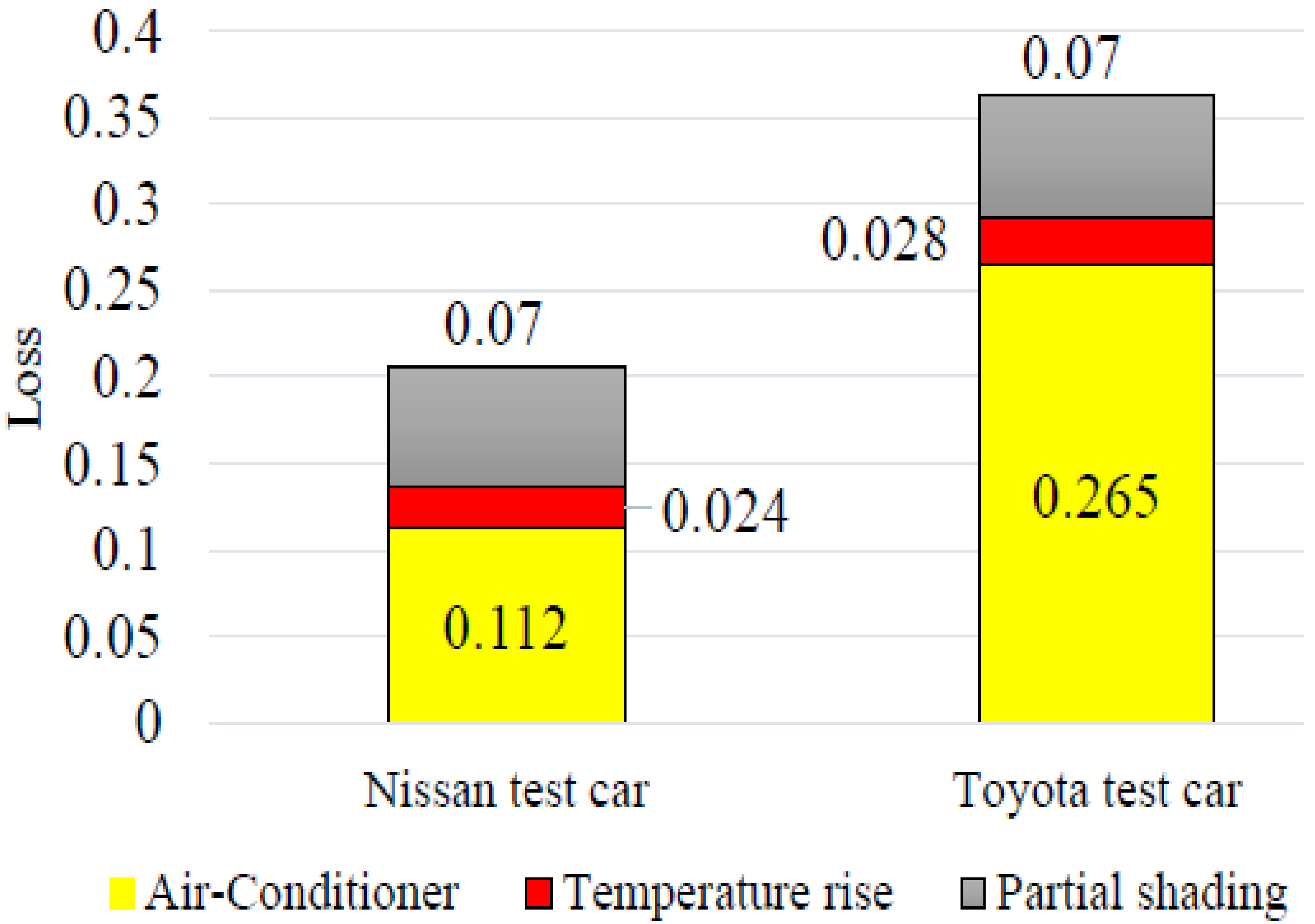

Analytical results of various power losses of SEV according to test driving by Toyota and Nissan test cars.

M. Yamaguchi et al., to be presented at the 41st EU-PVSEC, Vienna, Austria, Sep. 2024.